

Self-Supervised Learning of Graph Neural Networks: A Unified Review

Yaochen Xie, Zhao Xu, Jingtun Zhang, Zhengyang Wang, Shuiwang Ji, *Senior Member, IEEE*

Abstract—Deep models trained in supervised mode have achieved remarkable success on a variety of tasks. When labeled samples are limited, self-supervised learning (SSL) is emerging as a new paradigm for making use of large amounts of unlabeled samples. SSL has achieved promising performance on natural language and image learning tasks. Recently, there is a trend to extend such success to graph data using graph neural networks (GNNs). In this survey, we provide a unified review of different ways of training GNNs using SSL. Specifically, we categorize SSL methods into contrastive and predictive models. In either category, we provide a unified framework for methods as well as how these methods differ in each component under the framework. Our unified treatment of SSL methods for GNNs sheds light on the similarities and differences of various methods, setting the stage for developing new methods and algorithms. We also summarize different SSL settings and the corresponding datasets used in each setting. To facilitate methodological development and empirical comparison, we develop a standardized testbed for SSL in GNNs, including implementations of common baseline methods, datasets, and evaluation metrics.

Index Terms—Self-supervised learning, graph neural networks, deep learning, unsupervised learning, graph analysis, survey, review.

1 INTRODUCTION

A Deep model takes some data as its inputs and is trained to output desired predictions. A common way to train a deep model is to use the supervised mode in which a sufficient amount of input data and label pairs are given. However, since a large number of labels are required, the supervised training becomes inapplicable in many real-world scenarios, where labels are expensive, limited, or even unavailable. In such cases, self-supervised learning (SSL) enables the training of deep models on unlabeled data, removing the need of excessive annotated labels. When no labeled data is available, SSL serves as an approach to learn representations from unlabeled data itself. When a limited number of labeled data is available, SSL from unlabeled data can be used either as a pre-training process after which labeled data are used to fine-tune the pre-trained deep models for downstream tasks, or as an auxiliary training task that contributes to the performance of main tasks.

Recently, SSL has shown its promising capability in data restoration tasks, such as image super-resolution [1], image denoising [2, 3, 4], and single-cell analysis [5]. It has also achieved remarkable progress in representation learning for different data types, including language sequences [6, 7, 8], images [9, 10, 11, 12], and graphs with sequence models [13, 14] or spectral models [15]. The key idea of these methods is to define pretext training tasks to capture and use the dependencies among different dimensions of the input data, *e.g.*, the spatial, temporal, or channel dimensions, with robustness and smoothness. Taking the image domain as an example, Doersch et al. [16], Noroozi and Favaro [17],

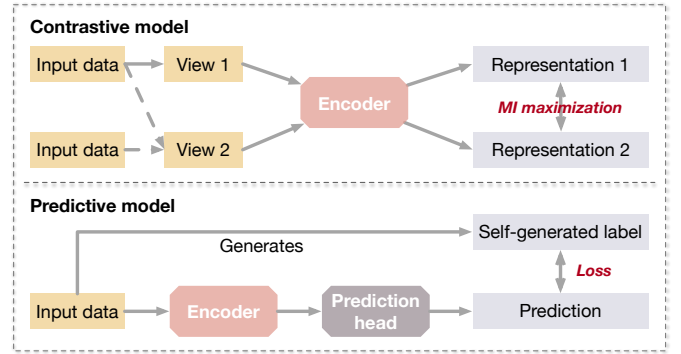


Fig. 1. A comparison between the contrastive model and the predictive model in general.

and He et al. [18] design different pretext tasks to train convolutional neural networks (CNNs) to capture relationships between different crops from an image. Chen et al. [10] and Grill et al. [19] train CNNs to capture dependencies between different augmentations of an image.

Based on how the pretext training tasks are designed, SSL methods can be divided into two categories; namely contrastive models and predictive models. The major difference between the two categories is that contrastive models require data-data pairs for training, while predictive models require data-label pairs, where the labels are self-generated from the data, as illustrated in Figure 1. Contrastive models usually utilize self-supervision to learn data representation or perform pre-training for downstream tasks. Given the data-data pairs, contrastive models perform discrimination between positive pairs and negative pairs. On the other hand, predictive models are trained in a supervised fashion, where the labels are generated based on certain properties of the input data or by selecting certain parts of the data.

- Y. Xie, Z. Xu, J. Zhang, and S. Ji are with Department of Computer Science & Engineering, Texas A&M University, College Station, TX 77843.
E-mail: {ethanyxc, zhaoxu, zjt6791, sji}@tamu.edu
- Z. Wang is with Amazon.com Services LLC, Seattle, WA 98109.
E-mail: zhengywa@amazon.com

Predictive models usually consist of an encoder and one or more prediction heads. When applied as a representation learning or pre-training method, the prediction heads of a predictive model are removed in the downstream task.

In graph data analysis, SSL can potentially be of great importance to make use of a massive amount of unlabeled graphs such as molecular graphs [20, 21]. With the rapid development of graph neural networks (GNNs) [22, 23, 24, 25, 26, 27, 28], basic components of GNNs [29, 30, 31, 32, 33, 34] and other related fields [35, 36] have been well studied and made substantial progress. In comparison, applying SSL on GNNs is still an emerging field. Due to the similarity in data structure, many SSL methods for GNNs are inspired by methods in the image domain, such as DGI [37] and graph autoencoders [38]. However, there are several key challenges in applying SSL on GNNs due to the uniqueness of the graph-structured data. To obtain good representations of graphs and perform effective pre-training, self-supervised models are supposed to capture essential information from both nodes attributes and structural topology of graphs [39]. For contrastive models, as the GPU memory issue of performing self-supervised learning is not a major concern for graphs, the key challenge lies in how to obtain good views of graphs and the selection of graph encoder for different models and datasets. For predictive models, it becomes essential that what labels should be generated so that the non-trivial representations are learned to capture information in both node attributes and graph structures.

To foster methodological development and facilitate empirical comparison, we review SSL methods of GNNs and provide unified views for both contrastive and predictive methods. Our unified treatment of this topic may shed light on the similarities and differences among current methods and inspire new methods. We also provide a standardized testbed as a convenient and flexible open-source platform for performing empirical comparisons. We summarize the contributions of this survey as follows:

- We provide thorough and up-to-date reviews on SSL methods for graph neural networks. To the best of our knowledge, our survey presents the first review of SSL specifically on graph data.
- We unify existing contrastive learning methods for GNNs with a general framework. Specifically, we unify the contrastive objectives from the perspective of mutual information. From this fresh view, different ways to perform contrastive learning can be considered as performing three transformations to obtain views. We review theoretical and empirical studies and provide insights to guide the choice of each component in the framework.
- We categorize and unify SSL methods with self-generated labels as predictive learning methods, and elucidate their connections and differences by different ways of obtaining labels.
- We summarize common settings of SSL tasks and commonly used datasets of various categories under different settings, setting the stage for developments of future methods.
- We develop a standardized testbed for applying SSL on GNNs, including implementations of common

baseline methods and benchmarks, enabling convenient and flexible customization for future methods.

An overview of self-supervised learning methods of different categories is given in Figure 2.

2 PROBLEM FORMULATION

2.1 Notations

We consider an attributed undirected graph $G = (V, E, \alpha)$, where $V = \{v_1, \dots, v_{|V|}\}$ denotes the set of its nodes, $E = \{e_1, \dots, e_{|E|}\}$ denotes the set of its edges and $\alpha : V \rightarrow \mathbb{R}^d$ denotes the mapping from a node to its attributes of d dimensions. For labeled graphs, we consider the one-hot vectors of their node labels as node attributes. We denote the adjacency matrix of G by $\mathbf{A} \in \mathbb{R}^{|V| \times |V|}$, where $\mathbf{A}_{ij} = \mathbb{1}[(v_i, v_j) \in E]$ for $1 \leq i, j \leq |V|$, and denote the feature matrix of G by $\mathbf{X} \in \mathbb{R}^{|V| \times d}$, where the i -th row $X_i = \alpha(v_i)$ for $1 \leq i \leq |V|$.

Given the graph data (\mathbf{A}, \mathbf{X}) from the input space \mathcal{G} , we are interested in the representation of the graph at either node-level or graph-level for any downstream prediction tasks. In general, we want to learn an encoder f such that the representation $\mathbf{H} = f(\mathbf{A}, \mathbf{X})$ can achieve desired performance on a downstream prediction task. For node-level prediction tasks, we learn a node-level encoder $f_n : \mathbb{R}^{|V| \times |V|} \times \mathbb{R}^{|V| \times d} \rightarrow \mathbb{R}^{|V| \times q}$ that takes the graph data (\mathbf{A}, \mathbf{X}) as inputs and computes the representations for all nodes $\mathbf{H}_{node} = f_{node}(\mathbf{A}, \mathbf{X}) \in \mathbb{R}^{|V| \times q}$. For graph-level prediction tasks, we learn a graph-level encoder $f_g : \mathbb{R}^{|V| \times |V|} \times \mathbb{R}^{|V| \times d} \rightarrow \mathbb{R}^q$ that computes a single vector $\mathbf{h}_{graph} = f_{graph}(\mathbf{A}, \mathbf{X}) \in \mathbb{R}^q$ as the representation of the given graph. Practically, graph-level encoders are usually constructed as a node-level encoder followed by a readout function. In many cases, a model for node-level representation learning may also be utilized to compute graph-level representations by adding an appropriate readout function, and *vice versa* (by removing the readout function).

We let \mathcal{P} denote the distribution of unlabeled graphs over the input space \mathcal{G} . Given a training dataset, the distribution \mathcal{P} can be simply constructed as the uniform distribution over samples in the dataset. The self-supervision can contribute to the learning of graph encoders f by utilizing information from \mathcal{P} and minimizing a self-supervised loss $\mathcal{L}_{ssl}(f, \mathcal{P})$ determined by a specifically designed self-supervised learning task.

2.2 Paradigms for Self-Supervised Learning

Typical training paradigms to apply the self-supervision include unsupervised representation learning, unsupervised pretraining, and auxiliary learning.

In **unsupervised representation learning**, only the distribution \mathcal{P} of unlabeled graphs is available for the entire training process. The problem of learning the representation of a given graph data $(\mathbf{A}, \mathbf{X}) \sim \mathcal{P}$ is formulated as

$$f^* = \arg \min_f \mathcal{L}_{ssl}(f, \mathcal{P}), \quad (1)$$

$$\mathbf{H}^* = f^*(\mathbf{A}, \mathbf{X}). \quad (2)$$

The learned representations \mathbf{H}^* are then used in further downstream tasks such as linear classification and clustering.

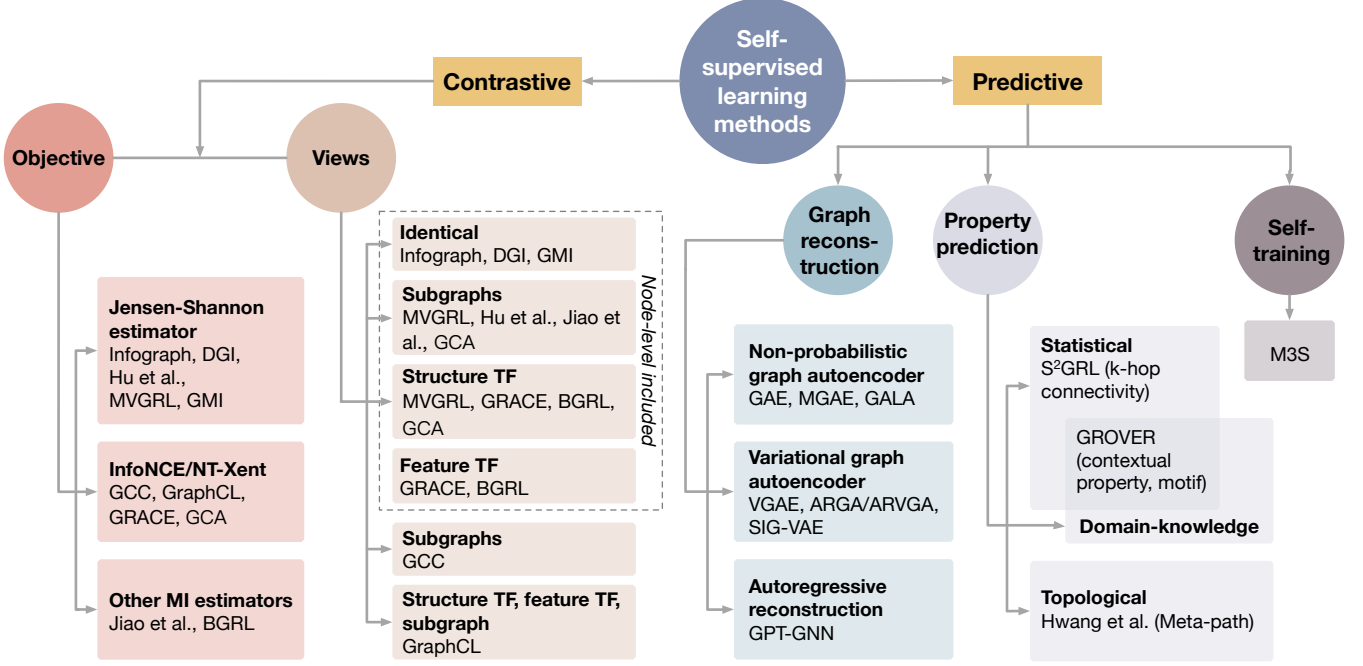


Fig. 2. An overview of self-supervised learning methods. We categorize self-supervised learning methods into two branches: contrastive methods and predictive methods. For contrastive methods, we further divide them regarding either views generation or objective. From the aspect of views generation, Infograph [40], DGI [37] and GMI [41] contrast views between nodes and graph; Hu et al. [42] and Jiao et al. [43] contrast views between nodes and subgraph; MVGRL [9] and GCA [44] contrast views between nodes and subgraph or structurally transformed graph; GRACE [45] and BGRL [46] contrast views between nodes and structurally transformed graph or featurally transformed graph. Above methods include node-level representation to generate local/global contrastive pairs. Dissimilarly, following methods use global representation only to generate global/global contrastive pairs. GCC [47] contrasts views between subgraphs; GraphCL [48] contrasts views of subgraphs and randomly transformed graphs. From aspect of objective, Infograph [40], DGI [37], Hu et al. [42], MVGRL [9] and GMI [41] employ Jensen-Shannon estimator; GCC [47], GraphCL [48], GRACE [45] and GCA [44] employ InfoNCE (NT-Xent); Jiao et al. [43] and BGRL [46] use other MI estimators. For the predictive methods, we further divide them into graph reconstruction, property prediction, and self-training. Under graph reconstruction, GAE [38], MGAE [49], and GALA [50] utilize the non-probabilistic graph autoencoder; VGAE [38], ARGA/ARVGA [51], and SIG-VAE [52] utilize variational graph autoencoder; GPT-GNN [53] applies autoregressive reconstruction. Under property prediction, S²GRL [54] performs the prediction of k-hop connectivity as a statistical property; GROVER [55] performs predictions of a statistical contextual property and a domain-knowledge involved property; Hwang et al. [56] predict a topological property, meta-path. M3S [57] employs self-training and node clustering to provide self-supervision.

The **unsupervised pretraining** is usually performed in a two-stage training [58]. It first trains the encoder f with unlabeled graphs. The pre-trained encoder f_{init} is then used as the initialization of the encoder in a supervised finetuning stage. Formally, in addition to the distribution \mathcal{P} , the learner further gains access to a distribution \mathcal{P} of labeled graphs over $\mathcal{G} \times \mathcal{Y}$, where \mathcal{Y} denotes the label space. Again, given the labeled training dataset, \mathcal{P} can be simply constructed as the uniform distribution over labeled samples in the dataset. The pretrained encoder f_{init} is then fine-tuned on \mathcal{P} , together with a prediction head h s.t. $h(f(\mathbf{A}, \mathbf{X})) \in \mathcal{Y}$ and a supervised loss \mathcal{L}_{sup} , i.e.,

$$f^*, h^* = \arg \min_{(f, h)} \mathcal{L}_{sup}(f, h, \mathcal{P}), \quad (3)$$

with initialization

$$f_{init} = \arg \min_f \mathcal{L}_{ssl}(f, \mathcal{P}). \quad (4)$$

The unsupervised pretraining and supervised finetuning paradigm is considered as the most strategy to perform semi-supervised learning and transfer learning. For semi-supervised learning, the labeled graphs in the finetuning dataset is a portion of the pretraining dataset. For transfer learning, the pretraining and finetuning datasets are from different domains. Note that a similar learning setting called

unsupervised domain adaptation has also been studied generally [59] or specifically in the image domain [60], where the encoder is pre-trained on labeled data but finetuned on unlabeled data under self-supervision. Since the paradigm is not specifically studied in the graph domain, we do not discuss the learning setting in detail in this survey.

The **auxiliary learning**, also known as joint training [58], aims to improve the performance of a supervised primary learning task by including an auxiliary task under self-supervision. Formally, we let \mathcal{Q} denote the joint distribution of graph data and labels for the primary learning task and \mathcal{P} denote the marginal of graph data. We want to learn both the decoder f and the prediction head h , where h is trained under supervision on \mathcal{Q} and f is trained under both supervision and self-supervision on \mathcal{P} . The learning problem is formulated as

$$f^*, h^* = \arg \min_{(f, h)} \mathcal{L}_{sup}(f, h, \mathcal{Q}) + \lambda \mathcal{L}_{ssl}(f, \mathcal{P}), \quad (5)$$

where λ is a positive scalar weight that balances the two terms in the loss.

3 CONTRASTIVE LEARNING

The study of contrastive learning has made significant progress in natural language processing and computer vi-

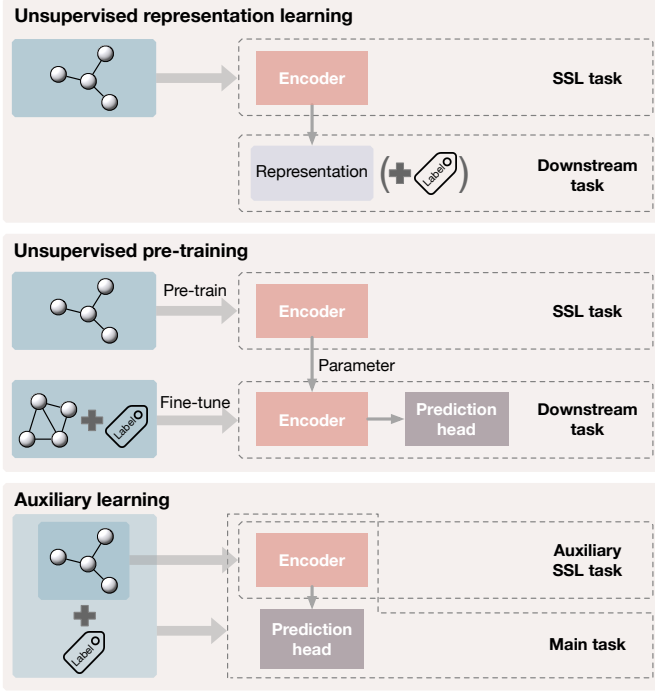


Fig. 3. Paradigms for self-supervised learning. **Top:** in unsupervised representation learning, graphs only are used to train the encoder through the self-supervised task. The learned representations are fixed and used in downstream tasks such as linear classification and clustering. **Middle:** unsupervised pre-training trains the encoder with unlabeled graphs by the self-supervised task. The pre-trained encoder’s parameters are then used as the initialization of the encoder used in supervised fine-tuning for downstream tasks. **Bottom:** in auxiliary learning, an auxiliary task with self-supervision is included to help learn the supervised main task. The encoder is trained through both the main task and the auxiliary task simultaneously.

sion. Inspired by the success of contrastive learning in images, recent studies propose similar contrastive frameworks to enable self-supervised training on graph data. Given training graphs, contrastive learning aims to learn one or more encoders such that representations of similar graph instances agree with each other, and that representations of dissimilar graph instances disagree with each other. We unify existing approaches to constructing contrastive learning tasks into a general framework that learns to discriminate jointly sampled view pairs (*e.g.* two views belonging to the same instance) from independently sampled view pairs (*e.g.* views belonging to different instances). In particular, we obtain multiple views from each graph in the training dataset by applying different transformations. Two views generated from the same instance are usually considered as a positive pair and two views generated from different instances are considered as a negative pair. The agreement is usually measured by metrics related to the mutual information between two representations.

One major difference among graph contrastive learning methods lies in (a) the objective for discrimination task given view representations. In addition, due to the unique data structure of graphs, graph contrastive learning methods also differ in (b) approaches that views are obtained, and (c) graph encoders that compute the representations of views. A graph contrastive learning method can be deter-

mined by specifying its components (a)–(c). In this section, we summarize graph contrastive learning methods in a unified framework and then introduce (a)–(c) individually used in existing studies.

3.1 Overview of Contrastive Learning Framework

In general, key components that specify a contrastive learning framework include transformations that compute multiple views from each given graph, encoders that compute the representation for each view, and the learning objective to optimize parameters in encoders. An overview of the framework is shown in Figure 4. Concretely, given a graph (A, X) as a random variable distributed from \mathcal{P} , multiple transformations $\mathcal{T}_1, \dots, \mathcal{T}_k$ are applied to obtain different views w_1, \dots, w_k of the graph. Then, a set of encoding networks f_1, \dots, f_k take corresponding views as their inputs and output the representations h_1, \dots, h_k of the graph from each views. Formally, we have

$$w_i = \mathcal{T}_i(A, X), \quad (6)$$

$$h_i = f_i(w_i), \quad i = 1, \dots, k. \quad (7)$$

We assume $w_i = (\hat{A}_i, \hat{X}_i) = \mathcal{T}_i(A, X)$ in this survey since existing contrastive methods consider their views as graphs. However, note that not all views w_i are necessarily graphs or sub-graphs in a general sense. In addition, certain encoders can be identical to each other or share their weights.

During training, the contrastive objective aims to train encoders to maximize the agreement between view representations computed from the same graph instance. The agreement is usually measured by the mutual information $\mathcal{I}(h_i, h_j)$ between a pair of representations h_i and h_j . We formalize the contrastive objective as

$$\max_{\{f_i\}_{i=1}^k} \frac{1}{\sum_{i \neq j} \sigma_{ij}} \left[\sum_{i \neq j} \sigma_{ij} \mathcal{I}(h_i, h_j) \right], \quad (8)$$

where $\sigma_{ij} \in \{0, 1\}$, and $\sigma_{ij} = 1$ if the mutual information is computed between h_i and h_j , and $\sigma_{ij} = 0$ otherwise, and h_i and h_j are considered as two random variables belonging to either a joint distribution or the product of two marginals. To enable efficient computation of the mutual information, certain estimators $\hat{\mathcal{I}}$ of the mutual information are usually used instead as the learning objective. Note that some contrastive methods apply projection heads [9, 48] to the representations. For the sake of uniformity, we consider such projection heads as parts of the computation in the mutual information estimation.

During inference, one can either use a single trained encoder to compute the representation or a combination of multiple view representations such as the linear combination or the concatenation as the final representation of a given graph. Three examples of using encoders in different ways during inference are illustrated in Figure 5.

3.2 Contrastive Objectives

3.2.1 Mutual Information Estimation

Given a pair of random variables (x, y) , the mutual information $\mathcal{I}(x, y)$ measures the information that x and y share,

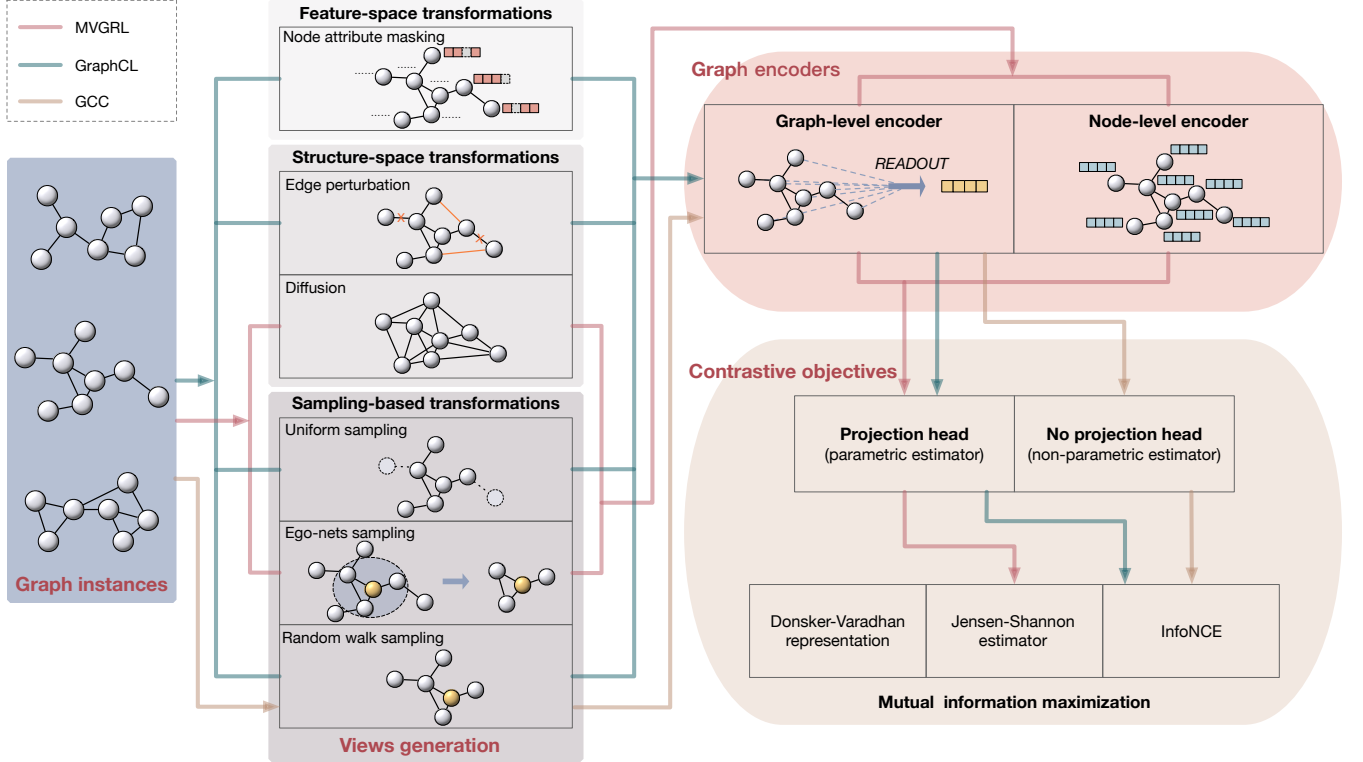


Fig. 4. The general framework of contrastive learning methods. A contrastive method can be determined by defining its views generation, encoders, and objective. Different views can be generated by a single or a combination of instantiations of three types of transformations. Commonly employed transformations include node attribute masking as feature transformation, edge perturbation and diffusion as structure transformations, and uniform sampling, ego-nets sampling, and random walk sampling as sample-based transformations. Note that we consider a node representation in node-graph contrast [12, 37, 40] as a graph view with ego-nets sampling followed by a node-level encoder. For graph encoders, most methods employ graph-level encoders and node-level encoders are usually used in node-graph contrast. For MI estimators as learning objectives, common options include Donsker-Varadhan representation, Jensen-Shannon estimator, InfoNCE, and other non-bound objectives. An estimator is parametric if projection heads are employed, and is non-parametric otherwise. Examples of three specific contrastive learning methods are illustrated in the figure. Red lines connect options used in MVGRL [9]; green lines connect options adopted in GraphCL [48]; yellow lines connect options taken in GCC [47].

given by

$$\mathcal{I}(\mathbf{x}, \mathbf{y}) = D_{KL}(p(\mathbf{x}, \mathbf{y}) || p(\mathbf{x})p(\mathbf{y})) \quad (9)$$

$$= \mathbb{E}_{p(\mathbf{x}, \mathbf{y})} \left[\log \frac{p(\mathbf{x}, \mathbf{y})}{p(\mathbf{x})p(\mathbf{y})} \right], \quad (10)$$

where D_{KL} denotes the Kullback-Leibler (KL) divergence. The contrastive learning seeks to maximize the mutual information between two views as two random variables. In particular, it trains the encoders to be contrastive between representations of a positive pair of views that comes from the joint distribution $p(\mathbf{v}_i, \mathbf{v}_j)$ and representations of a negative pair of views that comes from the product of marginals $p(\mathbf{v}_i)p(\mathbf{v}_j)$.

In order to computationally estimate and maximize the mutual information in the contrastive learning, three typical lower-bounds to the mutual information are derived [61], namely, the Donsker-Varadhan representation $\hat{\mathcal{I}}^{(DV)}$ [62, 63], the Jensen-Shannon estimator $\hat{\mathcal{I}}^{(JS)}$ [64] and the noise-contrastive estimation $\hat{\mathcal{I}}^{(NCE)}$ (InfoNCE) [11, 65]. Among the three lower-bounds, $\hat{\mathcal{I}}^{(JS)}$ and $\hat{\mathcal{I}}^{(NCE)}$ are commonly used as objectives in the contrastive learning in graphs.

A mutual information estimation is usually computed based on a discriminator $\mathcal{D} : \mathbb{R}^q \times \mathbb{R}^q \rightarrow \mathbb{R}$ that maps the representations of two views to an agreement score between

the two representations. The discriminator \mathcal{D} can be either parametric or non-parametric. For example, the discriminator can optionally apply a set of projection heads [9, 48] to the representations $\mathbf{h}_1, \dots, \mathbf{h}_k$ before computing the pairwise similarity. We formalize the optional projection heads as g_1, \dots, g_k such that

$$\mathbf{z}_i = g_i(\mathbf{h}_i), \quad i = 1, \dots, k, \quad (11)$$

where g_i can be an identical mapping, a linear projection or an MLP. Parameterized g_i are optimized simultaneously with the encoders f_i in Eqn. (8), given by

$$\max_{\{f_i, g_i\}_{i=1}^k} \frac{1}{\sum_{i \neq j} \sigma_{ij}} \left[\sum_{i \neq j} \sigma_{ij} \hat{\mathcal{I}}_{g_i, g_j}(\mathbf{h}_i, \mathbf{h}_j) \right], \quad (12)$$

We now introduce the three lower bounds as specific estimations of mutual information and a non-bound estimation of mutual information.

3.2.2 Donsker-Varadhan Estimator

The Donsker-Varadhan (DV) estimator, also known as the DV representation of the KL divergence, is a lower-bound to the mutual information and hence can be applied to

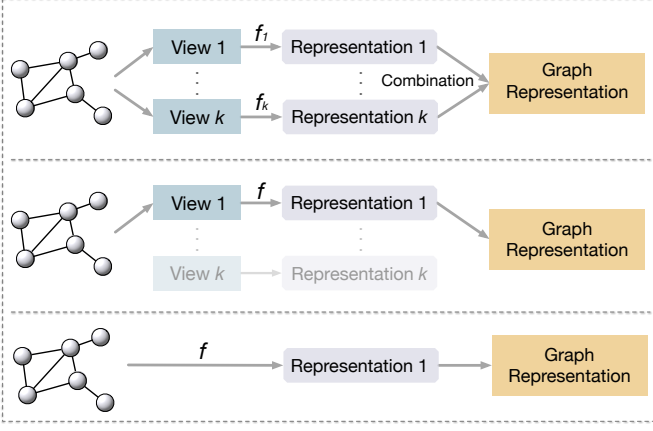


Fig. 5. Different ways of using encoders during inference. **Top**: encoders for multiple views are used and output representations are merged by combinations such as summation [9] or concatenation. **Middle**: only the main encoder [46] and the corresponding view are used during inference. **Bottom**: the given graph is directly input to the only encoder [47, 48] shared by all views to compute its representation.

maximize the mutual information. Given \mathbf{h}_i and \mathbf{h}_j , the lower-bound is computed as

$$\hat{\mathcal{I}}^{(DV)}(\mathbf{h}_i, \mathbf{h}_j) = \mathbb{E}_{p(\mathbf{h}_i, \mathbf{h}_j)}[\mathcal{D}(\mathbf{h}_i, \mathbf{h}_j)] - \log \mathbb{E}_{p(\mathbf{h}_i)p(\mathbf{h}_j)}[e^{\mathcal{D}(\mathbf{h}_i, \mathbf{h}_j)}], \quad (13)$$

where $p(\mathbf{h}_i, \mathbf{h}_j)$ denotes the joint distribution of the two representations $\mathbf{h}_i, \mathbf{h}_j$ and $p(\mathbf{h}_i)p(\mathbf{h}_j)$ denotes the product of marginals. For simplicity and to include the graph data distribution \mathcal{P} , we assume transformations \mathcal{T}_i to be deterministic and encoders f_i to be injective, and have $p(\mathbf{h}_i, \mathbf{h}_j) = p(\mathbf{h}_i)p(\mathbf{h}_j|\mathbf{h}_i) = p(f_i(\mathcal{T}_i(\mathbf{A}, \mathbf{X})))p(f_j(\mathcal{T}_j(\mathbf{A}, \mathbf{X}))|(\mathbf{A}, \mathbf{X}))$. We hence re-write Eqn. (13) as

$$\hat{\mathcal{I}}^{(DV)}(\mathbf{h}_i, \mathbf{h}_j) = \mathbb{E}_{(\mathbf{A}, \mathbf{X}) \sim \mathcal{P}}[\mathcal{D}(\mathbf{h}_i, \mathbf{h}_j)] - \log \mathbb{E}_{[(\mathbf{A}, \mathbf{X}), (\mathbf{A}', \mathbf{X}')] \sim \mathcal{P} \times \mathcal{P}}[e^{\mathcal{D}(\mathbf{h}_i, \mathbf{h}_j)}], \quad (14)$$

where \mathbf{h}_i and \mathbf{h}_j in the first term are computed from (\mathbf{A}, \mathbf{X}) distributed from \mathcal{P} , \mathbf{h}_i and \mathbf{h}_j' in the second term are computed from (\mathbf{A}, \mathbf{X}) and $(\mathbf{A}', \mathbf{X}')$ identically and independently distributed from \mathcal{P} , respectively. In following descriptions of other objectives, we use the later version that includes \mathcal{P} .

3.2.3 Jensen-Shannon Estimator

Compared to the Donsker-Varadhan estimator, the Jensen-Shannon (JS) estimator enables more efficient estimation and optimization of the mutual information by computing the JS-divergence between the joint distribution and the product of marginals.

Given two representations \mathbf{h}_i and \mathbf{h}_j computed from the random variable (\mathbf{A}, \mathbf{X}) and a discriminator \mathcal{D} , **DGI** [37], **InfoGraph** [40], Hu et al. [42] and **MVGRL** [9] computes the JS estimator

$$\hat{\mathcal{I}}^{(JS)}(\mathbf{h}_i, \mathbf{h}_j) = \mathbb{E}_{(\mathbf{A}, \mathbf{X}) \sim \mathcal{P}}[\log(\mathcal{D}(\mathbf{h}_i, \mathbf{h}_j))] + \mathbb{E}_{[(\mathbf{A}, \mathbf{X}), (\mathbf{A}', \mathbf{X}')] \sim \mathcal{P} \times \mathcal{P}}[\log(1 - \mathcal{D}(\mathbf{h}_i, \mathbf{h}_j'))], \quad (15)$$

where $\mathbf{h}_i, \mathbf{h}_j$ in the first term are computed from (\mathbf{A}, \mathbf{X}) distributed from \mathcal{P} , \mathbf{h}_i and \mathbf{h}_j' in the second term are

computed from (\mathbf{A}, \mathbf{X}) and $(\mathbf{A}', \mathbf{X}')$ identically and independently distributed from the distribution \mathcal{P} . To further include edge features, Peng et al. [41] derives the graphic mutual information (**GMI**) based on MI decomposition and optimizes GMI via JS estimator. Note that [40] and [9] depict a softplus version of the JS estimator,

$$\hat{\mathcal{I}}^{(JS-SP)}(\mathbf{h}_i, \mathbf{h}_j) = \mathbb{E}_{(\mathbf{A}, \mathbf{X}) \sim \mathcal{P}}[-sp(-\mathcal{D}'(\mathbf{h}_i, \mathbf{h}_j))] - \mathbb{E}_{[(\mathbf{A}, \mathbf{X}), (\mathbf{A}', \mathbf{X}')] \sim \mathcal{P} \times \mathcal{P}}[sp(\mathcal{D}'(\mathbf{h}_i, \mathbf{h}_j'))], \quad (16)$$

where $sp(x) = \log(1 + e^x)$. We consider the JS estimators in Eqn. (15) and Eqn. (16) to be equivalent by letting $\mathcal{D}(\mathbf{h}_i, \mathbf{h}_j) = \text{sigmoid}(\mathcal{D}'(\mathbf{h}_i, \mathbf{h}_j))$.

For the the negative pairs of graphs $[(\mathbf{A}, \mathbf{X}), (\mathbf{A}', \mathbf{X}')] \sim \mathcal{P} \times \mathcal{P}$ in particular, **DGI** [37] samples one graph (\mathbf{A}, \mathbf{X}) from the training dataset and applies a stochastic corruption \mathcal{C} to obtain $(\mathbf{A}', \mathbf{X}') = \mathcal{C}(\mathbf{A}, \mathbf{X})$. For node-level tasks, **MVGRL** [9] follows **DGI** to obtain negative samples by corrupting given graphs. **InfoGraph** [40] independently samples two graphs from the training dataset as a negative pair, which is followed by **MVGRL** for graph-level tasks. Discriminators in JS estimators usually compute the agreement score between two vectors by their inner product with sigmoid, i.e., $\mathcal{D}(\mathbf{h}_i, \mathbf{h}_j) = \text{sigmoid}(\mathbf{z}_i^T \mathbf{z}_j) = \text{sigmoid}(g_i(\mathbf{h}_i)^T g_j(\mathbf{h}_j))$.

3.2.4 InfoNCE

InfoNCE $\hat{\mathcal{I}}^{(NCE)}$ is another lower-bound to the mutual information \mathcal{I} . Given the representations \mathbf{h}_i and \mathbf{h}_j of two views of random variable (\mathbf{A}, \mathbf{X}) , the discriminator \mathcal{D} , and the number of negative samples N , the InfoNCE is formalized as

$$\begin{aligned} \hat{\mathcal{I}}^{(NCE)}(\mathbf{h}_i, \mathbf{h}_j) &= \mathbb{E}_{(\mathbf{A}, \mathbf{X}) \sim \mathcal{P}}[\mathcal{D}(\mathbf{h}_i, \mathbf{h}_j) - \\ &\quad \mathbb{E}_{\mathbf{K} \sim \mathcal{P}^N} \left[\log \sum_{(\mathbf{A}', \mathbf{X}') \in \mathbf{K}} \frac{e^{\mathcal{D}(\mathbf{h}_i, \mathbf{h}_j')}}{N} \middle| (\mathbf{A}, \mathbf{X}) \right]] \\ &= \mathbb{E}_{[(\mathbf{A}, \mathbf{X}), \mathbf{K}] \sim \mathcal{P} \times \mathcal{P}^N} \left[\log \frac{e^{\mathcal{D}(\mathbf{h}_i, \mathbf{h}_j)}}{\sum_{(\mathbf{A}', \mathbf{X}') \in \mathbf{K}} e^{\mathcal{D}(\mathbf{h}_i, \mathbf{h}_j')}} \right] \\ &\quad + \log N, \end{aligned} \quad (17)$$

where \mathbf{K} consists of N random variables identically and independently distributed from \mathcal{P} , $\mathbf{h}_i, \mathbf{h}_j$ are the representations of the i -th and j -th views of (\mathbf{A}, \mathbf{X}) , and \mathbf{h}_j' is the representation of the j -th view of $(\mathbf{A}', \mathbf{X}')$.

In practice, we compute the InfoNCE on mini-batches of size $N + 1$. For each sample \mathbf{x} in a mini-batch \mathbf{B} , we consider the set of the rest N samples as a sample of \mathbf{K} . We then discard the constant term $\log N$ in Eqn. (17) and minimize the loss

$$\mathcal{L}_{\text{InfoNCE}} = -\frac{1}{N+1} \sum_{\mathbf{x} \in \mathbf{B}} \left[\log \frac{e^{\mathcal{D}(\mathbf{h}_i, \mathbf{h}_j)}}{\sum_{\mathbf{x}' \in \mathbf{B} \setminus \{\mathbf{x}\}} e^{\mathcal{D}(\mathbf{h}_i, \mathbf{h}_j')}} \right]. \quad (18)$$

Intuitively, the optimization of InfoNCE loss aims to score the agreement between \mathbf{h}_i and \mathbf{h}_j of views from the same instance \mathbf{x} higher than between \mathbf{h}_i and \mathbf{h}_j' from the rest N negative samples $\mathbf{B} \setminus \{\mathbf{x}\}$. **GraphCL** [48] and **GRACE** [45] include additional contrast among the same view of different instances (i.e., \mathbf{h}_i and \mathbf{h}_i') or different nodes in the same

view (intra-view contrast [45]), leading to the optimization of lower bounds of InfoNCE, which are still lower bounds of MI.

Discriminators in typical InfoNCE compute the agreement score between two vectors by their inner product, i.e., $\mathcal{D}(\mathbf{h}_i, \mathbf{h}_j) = \mathbf{z}_i^T \mathbf{z}_j = g_i(\mathbf{h}_i)^T g_j(\mathbf{h}_j)$. A specific type of the InfoNCE loss, known as the NT-Xent [66] loss, includes normalization and a preset temperature parameter τ in the computation of discriminator \mathcal{D} in the InfoNCE loss, i.e., $\mathcal{D}(\mathbf{h}_i, \mathbf{h}_j) = g_i(\mathbf{h}_i)^T g_j(\mathbf{h}_j) / \tau$. The discriminator in You et al. [48] computes the agreement score between vectors with normalizations, i.e., $\mathcal{D}(\mathbf{h}_i, \mathbf{h}_j) = \frac{g_i(\mathbf{h}_i)^T g_j(\mathbf{h}_j) / \tau}{\|g_i(\mathbf{h}_i)\| \|g_j(\mathbf{h}_j)\|}$, where $\|\cdot\|$ denotes the ℓ_2 -norm. Moreover, the Bayesian Personalized Ranking (BPR) loss [67] used in Jiao et al. [43] is equivalent to the InfoNCE loss when letting $N = 1$ and $\mathcal{D}(\mathbf{h}_i, \mathbf{h}_j) = \mathbf{h}_i^T \mathbf{h}_j$.

3.2.5 Non-Bound Mutual Information Estimators

There are other objectives that have been used in some studies, and these objectives can also increase mutual information. However, these objectives are not provable lower-bounds to the mutual information, and optimizing these objectives does not guarantee the maximization of the mutual information.

For example, Jiao et al. [43] proposes to minimize the triplet margin loss [68], which is commonly used in deep metric learning [69]. Given representations $\mathbf{h}_i, \mathbf{h}_j$ and the discriminator \mathcal{D} , the triplet margin loss is formalized as

$$\mathcal{L}_{\text{triplet}} = \mathbb{E}_{[(\mathbf{A}, \mathbf{X}), (\mathbf{A}', \mathbf{X}')] \sim \mathcal{P} \times \mathcal{P}} [\max\{\mathcal{D}(\mathbf{h}_i, \mathbf{h}_j) - \mathcal{D}(\mathbf{h}_i, \mathbf{h}'_j) + \epsilon, 0\}], \quad (19)$$

where $\mathcal{D}(\mathbf{h}_i, \mathbf{h}_j) = \text{sigmoid}(\mathbf{h}_i^T \mathbf{h}_j)$ and ϵ is the margin value.

Inspired by BYOL [19], BGRL [46] eliminates the need of negative samples by including a parametric predictor p_θ and minimize the loss

$$\mathcal{L}_{\text{BYOL}} = \mathbb{E}_{\mathbf{B} \sim \mathcal{P}^N} \left[-\frac{2}{N} \sum_{\mathbf{x} \in \mathbf{B}} \frac{[p_\theta(\mathbf{h}_i)]^T \mathbf{h}_j}{\|p_\theta(\mathbf{h}_i)\| \|\mathbf{h}_j\|} \right]. \quad (20)$$

As no negative sample is included, certain mechanisms and restrictions (such as updating an offline encoder with exponential moving average [19] and batch normalization) are required in the framework to prevent degenerate solutions and achieve similar effect of optimizing MI bound objectives.

3.2.6 Projection Head: Parametric Estimation

Many contrastive learning studies [9, 40, 48] propose to include projection heads g_i when computing the MI estimations. For example, Hassani and Khasahmadi [9], Sun et al. [40] use 3-layer MLPs, You et al. [48] use 2-layer MLPs as the projection heads and Sun et al. [40] applies a linear projection to the graph-level representation. The projection heads are shown to significantly improve the contrastive learning performance [10]. We consider MI estimators that include projection heads as parametric estimators and those without projection heads as non-parametric estimators. Then a reasonable explanation to the observation that the contrastive methods with projection heads usually achieve better performance is that parametric estimators provide better estimation to the mutual information.

3.2.7 Comparison and Discussion of Different Objectives

Among all contrastive objectives for graphs, the JS estimator $\hat{\mathcal{I}}^{(JS)}$ and InfoNCE $\hat{\mathcal{I}}^{(NCE)}$ based on lower-bounds to mutual information are most commonly used. Regarding the two estimators generally, Hjelm et al. [61] empirically shows that InfoNCE generally outperforms the JS estimator in most cases. However, compared to the JS estimator, InfoNCE is more sensitive to the number of negative samples N and requires a large number of negative samples in order to be competitive. Consequently, when the number of negative samples, i.e., the mini-batch size, is limited, the performance of InfoNCE could be limited and the JS estimator may become a better choice.

In addition, Hassani and Khasahmadi [9] perform ablation studies comparing the three objectives $\hat{\mathcal{I}}^{(DV)}$, $\hat{\mathcal{I}}^{(JS)}$ and $\hat{\mathcal{I}}^{(NCE)}$ with batch size ranged from 32 to 256 for graph classification and ranged from 2 to 8 for node classification. They show that the JS estimator generally leads to the best performance among all objectives on graph classification datasets, while InfoNCE (or NT-Xent) achieves overall best performance on node-classification tasks.

Moreover, Jiao et al. [43] compares the non-bound based triplet margin loss, the logistic loss [70] as an equivalence of the JS estimator and the BPR loss as an equivalence of the InfoNCE with $N = 1$ under their graph contrastive framework. Their results show that the JS estimator and the BPR loss (the InfoNCE loss with $N = 1$) are similarly effective in their method, while the triplet margin loss achieves the best performance among the three objectives. The results indicate that the triplet margin loss can still be effective, given some certain views of the graphs, when the positive pairs and negative pairs should not be discriminated absolutely.

3.3 Graph View Generation

To generate views from a graph sample distributed from \mathcal{P} , one usually applies different types of graph transformations (or augmentations) \mathcal{T} . Here, we only consider cases where \mathcal{T} still outputs the graph-structured data. We summarize the existing transformations applied to graph data in three categories, feature transformations, structure transformations and sampling-based transformations. Feature transformations can be formalized as

$$\mathcal{T}_{\text{feat}}(\mathbf{A}, \mathbf{X}) = (\mathbf{A}, \mathcal{T}_X(\mathbf{X})), \quad (21)$$

where $\mathcal{T}_X : \mathbb{R}^{|V| \times d} \rightarrow \mathbb{R}^{|V| \times d}$ performs the transformation on the feature matrix \mathbf{X} . Structure transformations can be formalized as

$$\mathcal{T}_{\text{struct}}(\mathbf{A}, \mathbf{X}) = (\mathcal{T}_A(\mathbf{A}), \mathbf{X}), \quad (22)$$

where $\mathcal{T}_A : \mathbb{R}^{|V| \times |V|} \rightarrow \mathbb{R}^{|V| \times |V|}$ performs the transformation on the adjacency matrix \mathbf{A} . And the sampling-based transformations are in the form

$$\mathcal{T}_{\text{sample}}(\mathbf{A}, \mathbf{X}) = (\mathbf{A}[S; S], \mathbf{X}[S]), \quad (23)$$

where $S \subseteq V$ denotes a subset of nodes and $[\cdot]$ selects certain rows (and columns) from a matrix based on indices of nodes in S . We consider the transformations applied in the existing contrastive learning methods to generate different views as a single or a combination of instantiations of the three

types of transformations above. Note that when node-level representations are of interest, the node-level contrasts are usually included. We consider nodes representations to be computed from views generated by ego-nets sampling from given graphs.

3.3.1 Feature Transformations

Given an input graph (\mathbf{A}, \mathbf{X}) , a feature transformation only performs transformation to the attribute matrix \mathbf{X} , i.e., $\mathcal{T}(\mathbf{A}, \mathbf{X}) = (\mathbf{A}, \mathcal{T}_X(\mathbf{X}))$.

Node attribute masking [48] is one of the most common way to apply the feature transformations. The node attribute masking randomly masks a small portion of attributes of all node with constant or random values. Concretely, given the input attribute matrix \mathbf{X} , we specify $\mathcal{T}_X(\mathbf{X})$ for the node attribute masking as

$$\mathcal{T}_X^{(mask)}(\mathbf{X}) = \mathbf{X} * (\mathbf{1} - \mathbf{1}_m) + \mathbf{M} * \mathbf{1}_m, \quad (24)$$

where $*$ denotes the element-wise multiplication, \mathbf{M} denotes a matrix with masking values and $\mathbf{1}_m$ denotes the masking location indicator matrix. Given the masking ratio r , elements in $\mathbf{1}_m$ are set to 1 individually with a probability r and 0 with a probability $1 - r$. To employ adaptive masking, Zhu et al. [44] propose to sample $\mathbf{1}_m$ with centrality-based probabilities, including degree centrality, eigenvector centrality, and PageRank centrality. The values in \mathbf{M} specifies different masking strategies. For example, $\mathbf{M} = \mathbf{0}$ applies a constant masking, $\mathbf{M} \sim N(\mathbf{0}, \Sigma)$ replaces the original values by Gaussian noise and $\mathbf{M} \sim N(\mathbf{X}, \Sigma)$ adds Gaussian noise to the original values.

In addition to contrastive models such as [48], attributes masking is also commonly applied in predictive models [2, 5] for regularized reconstruction. The node attribute masking forces the encoders to captures better dependencies between the masked attributes and unmasked context attributes and recover the masked value from its context during encoding.

3.3.2 Structure Transformations

Given an input graph (\mathbf{A}, \mathbf{X}) , a structure transformation only performs transformation to the adjacency matrix \mathbf{A} and remains \mathbf{X} to be the same, i.e., $\mathcal{T}(\mathbf{A}, \mathbf{X}) = (\mathcal{T}_A(\mathbf{A}), \mathbf{X})$. Existing contrastive methods apply two types of structure transformations, edge perturbation that randomly adds or drops edges between pairs of nodes and graph diffusion that creates new edges based on the accessibility from one node to another.

Edge perturbation [47, 48] randomly adds or drops edges in a given graph. Similarly to the node attribute masking, it applies masks to the adjacency matrix \mathbf{A} . In particular, we have

$$\mathcal{T}_A^{(pert)}(\mathbf{A}) = \mathbf{A} * (\mathbf{1} - \mathbf{1}_p) + (\mathbf{1} - \mathbf{A}) * \mathbf{1}_p, \quad (25)$$

where $*$ denotes the element-wise multiplication and $\mathbf{1}_p$ denotes the perturbation location indicator matrix. Given the perturbation ratio r , elements in $\mathbf{1}_p$ are set to 1 individually with a probability r and 0 with a probability $1 - r$. In addition, $\mathbf{1}_p$ is a symmetric matrix.

Diffusion [9] creates new connections between nodes based on random walks, aiming at generating a global

view (\mathbf{S}, \mathbf{X}) of the graph in contrast to the local view (\mathbf{A}, \mathbf{X}) . Two instantiations of diffusion transformations are proposed to use in [9], namely, the heat kernel $\mathcal{T}_A^{(heat)}$ and the Personalized PageRank $\mathcal{T}_A^{(PPR)}$, formulated as follows.

$$\mathcal{T}_A^{(heat)}(\mathbf{A}) = \exp(t\mathbf{A}\mathbf{D}^{-1} - t), \quad (26)$$

$$\mathcal{T}_A^{(PPR)}(\mathbf{A}) = \alpha \left(\mathbf{I}_n - (1 - \alpha)\mathbf{D}^{-1/2}\mathbf{A}\mathbf{D}^{-1/2} \right)^{-1}, \quad (27)$$

where $\mathbf{D} \in \mathbb{R}^{|V| \times |V|}$ is a diagonal degree matrix, α denotes the teleport probability in a random walk and t denotes the diffusion time.

Centrality-based edge removal [44] randomly removes edges based on pre-computed probabilities determined by the centrality score of each edge. Centrality-based probabilities for edge removal reflects the importance of each edge, where less important edges are more likely to be removed. In particular, the centrality score of an edge $(u, v) \in E$ is computed as $w_{uv} = (\phi_c(u) + \phi_c(v))/2$, where $\phi_c(u)$ and $\phi_c(v)$ are the centrality of nodes u and v connected by the edge and a higher centrality score leads to lower probability p_{uv} of edge removal.

3.3.3 Sampling-Based Transformations

We consider sampling-based transformations that sample node-induced sub-graphs from a given graph (\mathbf{A}, \mathbf{X}) , i.e., $\mathcal{T}_{\text{sample}}(\mathbf{A}, \mathbf{X}) = (\mathbf{A}[S; S], \mathbf{X}[S])$ with $S \subseteq V$. Note that more generalized sub-graph sampling methods that sample both nodes from V and edges from E can be considered as a combination of the node-induced sub-graph sampling and the edge perturbation. As different sampling-based transformations are determined by the set S of sampled nodes from the node-set V , we categorize the sampling-based transformations by how the set S is obtained. Existing contrastive methods apply three approaches to obtain the node subset S , uniform sampling, random walk sampling, and ego-nets sampling.

Uniform sampling and nodes dropping can be considered as the two simplest sampling-based transformation approaches. The transformation in [9] samples sub-graphs by uniformly sampling a given number of nodes S from V and edges of the sampled nodes. In addition, transformation methods in [48] include node dropping as one of the graph transformations, where each node has a certain probability to be dropped from the graph. We denote the set of dropped nodes by D and we have $S = V \setminus D$.

Ego-nets sampling can be considered as a sampling-based transformation to unify the contrast performed between graph-level representation and node-level representations in the general contrastive learning framework, such as in DGI [37], InfoGraph [40] and MVGRL [9]. In other words, we consider that node-level representations are computed by node-level encoders from certain views, namely, ego-nets, of a given graph. Given a typical graph encoder with L layers, the computation of the representation of each node v_i only depends on its L -hop neighborhood, also known as the L -ego-net of node v_i . We hence consider the computing of node-level representations as performing L -ego-net sampling and a node-level encoder with L layers.

In particular, for each node v_i in a given graph, the transformation \mathcal{T}_i samples the L -ego net surrounding node v_i as the view w_i , computed as

$$w_i = \mathcal{T}_i(\mathbf{A}, \mathbf{X}) = (\mathbf{A}[\mathcal{N}_L(v_i); \mathcal{N}_L(v_i)], \mathbf{X}[\mathcal{N}_L(v_i)]), \quad (28)$$

$$\mathcal{N}_L(v_i) = \{v : d(v, v_i) \leq L\} \quad (29)$$

where L denotes the number of layers in the node-level encoder f_i , d denotes the shortest distance between two nodes and $(\mathbf{A}[\cdot; \cdot], \mathbf{X}[\cdot])$ selects a sub-graph from (\mathbf{A}, \mathbf{X}) .

Random walk sampling is proposed in GCC [47] to sample sub-graphs based on random walks starting from a given node. The subset of nodes $S \in V$ is collected iteratively. At each iteration, the walk has a probability p_{ij} to travel from node v_i to node v_j and has a probability of $p_r = 0.8$ to return to the start node. GCC considers the random walk sampling with restart as a further transformation of the r -ego-net centered at the start node. Given the center (start) node, the random walk sampling can be hence considered as a stronger sampling-based transformation than the ego-nets sampling.

3.3.4 Discussions of Graph View Generation

Currently, there is no theoretical analysis guiding the generation of the view for graphs. However, Tian et al. [71] theoretically and empirically analyze the problem in a general view and image domain, considering the generation of the view from the aspect of mutual information. In particular, a good view generation should minimize the MI between two views $I(v_1, v_2)$, subject to $I(v_1, y) = I(v_2, y) = I(x, y)$. Intuitively, to guarantee that contrastive learning works, the generated views v_i should not affect the information that determines the prediction for the downstream task, under which restriction, stronger disagreement between views leads to better learning results. From the manifold point of view, a recent analytic study [72] proposes the expansion assumption and explains the data augmentation as to prompt the continuity in the neighborhood for each instance. It indicates similar requirements for the view generating by augmentation, *i.e.*, subject to that the neighborhood an instance does not intersect the neighborhood of instances that belong to the other class in the downstream task, a larger neighborhood of an instance could be more beneficial.

To this end, the learning on datasets with different downstream tasks may benefit from different types of transformations. For example, the property of a social network to be predicted in a downstream task may be more tolerant of minor changes in node attributes, for which the feature transformations can be more suitable. On the other hand, the property of a molecule usually depends on bonds in some functional groups, for which the edge perturbation may harm the learning while the sub-graph sampling could help. Empirically, You et al. [48] observes similar results. For example, edge perturbation is found contributory to the performance on social network datasets but harmful to some molecule data.

3.4 Graph Encoders

Graph encoders are usually constructed based on graph neural networks (GNNs) following a neighborhood aggregation strategy, where the representation of a node is

iteratively updated by combining the its own representation with the aggregated representation over its neighbors. Formally, the k -th layer of GNN is:

$$\mathbf{x}_v^{(k)} = \text{COMBINE}^{(k)}(\mathbf{x}_v^{(k-1)}, \mathbf{a}_v^k), \quad (30)$$

$$\mathbf{a}_v^k = \text{AGGREGATE}^{(k)}\left(\left(\mathbf{x}_u^{(k-1)}, \mathbf{x}_u^{(k-1)}\right) : u \in \mathcal{N}(v)\right), \quad (31)$$

where $\mathbf{x}_v^{(k)}$ denotes the feature vector of node v at the k -th layer, and $\mathcal{N}(v)$ is a set of neighbor nodes of v . Graph encoders mainly differ from their aggregation strategies. $\text{COMBINE}^{(k)}(\cdot)$ and $\text{AGGREGATE}^{(k)}(\cdot)$ are component functions that determine types of GNNs, such as Graph Convolutional Networks (GCNs) [22], Graph Attention Networks (GATs) [73] and Graph Isomorphism Networks (GINs) [23].

3.4.1 Node-Level and Graph-Level Representations

The most straight-forward way to obtain the node-level representation \mathbf{h}_v for node v is to directly use the node feature at the final layer K of the encoder [37, 42, 43], *i.e.*, $\mathbf{h}_v = \mathbf{x}_v^{(K)}$. One may also adopt skip connections or jumping knowledge [74] to generate node-level representation. However, the node-level representation produced by concatenating node features from all layers have different dimension from node features. To avoid such inconsistency in vector dimension, [40, 48] and [9] concatenate node features of all layers, followed by a linear transformation:

$$\mathbf{h}_v = \text{CONCAT}([\mathbf{x}_v^{(k)}]_{k=1}^K) \mathbf{W}, \quad (32)$$

where $\mathbf{W} \in \mathbb{R}^{(\sum_k d_k) \times d}$ is the weight matrix used to shrink the dimension size of \mathbf{h}_v .

The READOUT function is considered as the key operation to compute the graph-level representation $\mathbf{h}_{\text{graph}}$ given the node-level representations \mathbf{H} of the graph. For the sake of node permutation invariance, summation and averaging are most commonly used READOUT functions. Sun et al. [40], You et al. [48] and Hassani and Khasahmadi [9] employ sum over all the nodes' representations as

$$\mathbf{h}_{\text{graph}} = \text{READOUT}(\mathbf{H}) = \sigma\left(\sum_{v=1}^{|V|} \mathbf{h}_v\right), \quad (33)$$

where $|V|$ denotes the total number of nodes in the given graph, and σ is either sigmoid function, multi-layer perceptron or identity function. Veličković et al. [37] and Jiao et al. [43] employ mean pooling READOUT that averages all the node-level representations as

$$\mathbf{h}_{\text{graph}} = \text{READOUT}(\mathbf{H}) = \sigma\left(\frac{1}{|V|} \sum_{v=1}^{|V|} \mathbf{h}_v\right). \quad (34)$$

3.4.2 Effects of Graph Encoders

Typically, GNN-based encoders are not constrained on choices of GNN types and most frameworks [9, 47] allow various choices. However, some studies have more thorough considerations of GNN types. InfoGraph [40] adopts GIN to achieve less inductive bias for graph-level applications. GraphCL [48] finds GIN outperforms GCN and GAT in semi-supervised learning on node classification tasks. Hu et al. [42] observe that the most expressive GIN achieves

the best performance with pre-training, although GIN has slightly inferior performance than the less expressive GNNs without pre-training. That is, GIN achieves the highest performance gain of pre-training. This observation agrees with [75] that fully-utilization of pre-training requires an expressive model as limited expressive models can harm performance and the observation [76] that the quality of learned representations is impacted more by the choice of encoder than the objective. On the contrary, for SUBGCN [43], GCN-based encoders outperform other GNN-based encoders as GCN is more suitable to handle sub-graphs than more expressive GIN and GAT. In addition, Veličković et al. [37] and Zhu et al. [45] employ different encoders on different learning tasks, *i.e.*, GCN for transductive learning tasks, GraphSage-GCN or a mean-pooling layer with skip connection for inductive learning on large Reddit, and mean-pooling layers with skip or dense skip connections for inductive learning on multiple graphs PPI. These observations imply that different contrastive learning frameworks and methods may prefer distinct GNN types for encoders. Even for the same framework, encoder choices may vary when applying to different datasets.

4 PREDICTIVE LEARNING

Compared with contrastive learning methods, predictive learning methods train the graph encoder f together with a prediction head g under the supervision of informative labels self-generated for free. We use the term “predictive” instead of “generative” categorized by Liu et al. [77] to avoid confusion, as not all methods introduced in this section are necessarily generative models. Categorized by how the prediction targets are obtained, we summarize predictive learning frameworks for graphs into (1) graph reconstruction that learns to reconstruct certain parts of given graphs, (2) graph property prediction that learns to model non-trivial properties of given graphs, and (3) multi-stage self-training with pseudo-labels. In this section, we let $\mathbf{H} \in \mathbb{R}^{|V| \times q}$ denote the desired node-level representation and \mathbf{h}_i denote the representation of node v_i . The general frameworks of three types of predictive learning methods are shown in Figure 6.

4.1 Graph Reconstruction

Graph reconstruction provides a natural self-supervision for the training of graph neural networks. The prediction targets in graph reconstruction are certain parts of the given graphs such as the attribute of a subset of nodes or the existence of edge between a pair of nodes. In graph reconstruction tasks, the prediction head g is usually called the decoder which reconstructs a graph from its representation.

4.1.1 Non-Probabilistic Graph Autoencoders

The autoencoders, firstly proposed in [78], have been widely applied for the learning of data representations. Given the success in the image domain and natural language modeling, various variations of graph autoencoder [79] are proposed to learn graph representations. Aiming at learning the graph encoder f , graph autoencoders are trained to reconstruct certain parts of an input graph, given restricted

access to the graph or under certain regularization to avoid identical mapping.

GAE [38] represents the simplest version of the graph autoencoders. It performs the reconstruction on the adjacency matrix \mathbf{A} from the input graph (\mathbf{A}, \mathbf{X}) . Formally, it computes the reconstructed adjacency matrix $\hat{\mathbf{A}}$ by

$$\hat{\mathbf{A}} = g(\mathbf{H}) = \sigma(\mathbf{H}\mathbf{H}^T), \quad (35)$$

$$\mathbf{H} = f(\mathbf{A}, \mathbf{X}), \quad (36)$$

and is optimized by the binary cross-entropy loss between $\hat{\mathbf{A}}$ and \mathbf{A} . As GAE is originally proposed to learn node-level representations for link prediction problem, it assumes two linked nodes should have similar representations. **GraphSAGE** [80] introduces a similar framework with the self-supervision of the adjacency matrix based on a different objective including negative sampling. In addition, a recent work **SuperGAT** [81] includes the GAE objective as a self-supervised auxiliary loss during training a graph attention network to guide the learning of more expressive attention operators. Similarly, **SimP-GCN** [82] applies node-pair similarity as a substitute of the adjacency matrix to construct a self-supervised auxiliary task.

MGAE [49] follows the idea of **denoising autoencoder** [83]. Given a graph (\mathbf{A}, \mathbf{X}) , MGAE performs reconstructions on multiple randomly corrupted feature matrices $\{\tilde{\mathbf{X}}_i\}_{i=1}^m$ with a single-layer autoencoder f_θ and the objective

$$\sum_{i=1}^m \|\mathbf{X} - f_\theta(\mathbf{A}, \tilde{\mathbf{X}}_i)\|^2 + \lambda \|\theta\|^2, \quad (37)$$

where θ denotes the weights in the single-layer encoder, λ denotes the hyper-parameter for l^2 -regularization, and $\mathbf{H}_i := f_\theta(\mathbf{A}, \tilde{\mathbf{X}}_i)$ is considered as the reconstructed representation. To enable non-linearity, [49] proposes to stack multiple single-layer autoencoders. Formally, given the reconstructed representation $\mathbf{H}^{(\ell-1)}$ at the $(\ell-1)$ -th layer, the ℓ -th layer is trained by optimizing

$$\sum_{i=1}^m \|\mathbf{H}^{(\ell-1)} - \mathbf{H}_i^{(\ell)}\|^2 + \lambda \|\theta_\ell\|^2, \quad (38)$$

$$\mathbf{H}_i^{(\ell)} = f_{\theta_\ell}(\mathbf{A}, \tilde{\mathbf{H}}_i^{(\ell-1)}), \quad (39)$$

where $\tilde{\mathbf{h}}_i^{(\ell-1)}$ denotes the corrupted representation from the $(\ell-1)$ -th layer. The reconstructed representation at the last layer is then considered as the representation for downstream tasks.

GALA [50] introduces a multi-layer autoencoder with symmetric encoder and decoder, unlike GAE and MGAE. Motivated by the Laplacian smoothing [84] effect of GCN encoders, GALA designs the decoder by performing Laplacian sharpening [84], which prompts the decoded representation of each node to be dissimilar to the centroid of its neighbors. A Laplacian sharpening layer in the decoder g is computed by

$$\hat{\mathbf{X}}^{(\ell)} = 2\hat{\mathbf{X}}^{(\ell-1)} - \mathbf{D}^{-1}\mathbf{A}\hat{\mathbf{X}}^{(\ell-1)}, \quad (40)$$

where $\hat{\mathbf{X}}^{(\ell)}$ and $\hat{\mathbf{X}}^{(\ell-1)}$ denote the decoded representation and \mathbf{D} denotes the degree matrix. GALA reconstructs the

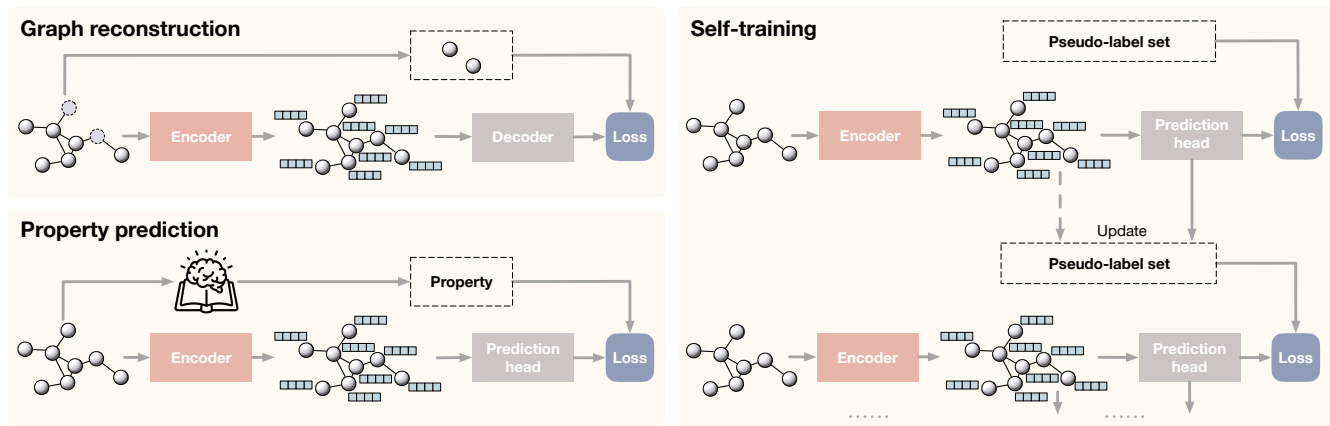


Fig. 6. Illustrations of three predictive learning frameworks. For predictive learning methods, self-generated labels provide self-supervision to train the encoder together with prediction heads (or the decoder). We conclude predictive learning methods into three categories by how the prediction targets are obtained. **Top left:** the prediction targets in graph reconstruction are certain parts of given graphs. For example, GAE [38] performs reconstruction on the adjacency matrix, and MGAE [49] performs reconstruction on randomly corrupted node attributes. **Bottom left:** the prediction targets in property prediction models are implicit and informative properties of given graphs. For example, S²GRL [54] predicts k-hop connectivity between two given nodes. Moreover, GROVER [55] utilizes motifs (functional groups) of molecules based on domain-knowledge as prediction targets. **Right:** the prediction targets in self-training are pseudo-labels. In M3S [57], the graph neural network is trained iteratively on a pseudo-label set initialized as the set of given ground-truth labels. Clustering and prediction are conducted to update the pseudo-label set based on which a fresh graph neural network is then trained. Such operations are performed multiple times as multi-stage.

feature matrix by optimizing the mean squared error $\|\hat{X} - X\|^2$ with

$$\hat{X} = g(A, H), \quad H = f(A, X). \quad (41)$$

Attribute masking [42], also referred to as **graph completion** [85], is another strategy to pre-train graph encoder f under the graph autoencoder framework by reconstructing masked node attributes. The encoder f computes the node-level representations H given the graph with its node attributes randomly masked. And a linear projection is applied to H as the decoder g to reconstruct the masked attributes. When the edge attributes are also available, one can also perform reconstruction on the masked edge attributes. Although the attribute masking is not explicitly named as graph autoencoders, we categorize it as graph autoencoders since the encoders are trained by performing reconstruction on the entire or certain parts of the input graph.

4.1.2 Variational Graph Autoencoders

Although sharing a similar encoder-decoder structure with standard autoencoders, variational autoencoders as generative models are built upon a different mathematical foundation assuming an existing prior distribution of latent representation that generates the observed data. Primarily targeted in learning the generation of the observed data, variational graph autoencoders also shown promising performance in learning good graph representations.

VGAE [38] introduces the simplest version of variational graph autoencoders. VGAE performs reconstruction on the adjacency matrix and is composed a inference model (encoder) $q(H|A, X) = \prod_{i=1}^{|V|} \mathcal{N}(h_i|\mu_i(A, X), \Sigma_i(A, X))$ parameterized by graph neural networks μ, Σ and a generative model (decoder) $p(A|H)$ modeled by the inner product of latent variables. VGAE optimizes the variational lower bound

$$\mathbb{E}_{q(H|A, X)} [\log p(A|H)] - \text{KL}[q(H|A, X)||p(H)], \quad (42)$$

where $\text{KL}(\cdot)$ denotes the KL-divergence and $p(H)$ denotes the prior given by the Gaussian distribution.

ARGA/ARVGA [51] propose to regularize the autoencoder with an adversarial network [86] which enforces the distribution of the latent variable to match the Gaussian prior. In addition to the encoder and decoder, a discriminator is trained to distinguish fake data generated by the encoder and the real data sampled from the Gaussian distribution. As the adversarial regularization is provably an equivalence of the JS-divergence between the distribution of the latent variable and the Gaussian prior, ARGA/ARVGA can achieve a similar effect to VGAE but with stronger regularization.

SIG-VAE [52] replace the inference model in the variational graph autoencoder a hierarchy of multiple stochastic layers to enable more flexible model of the latent variable. In particular, the inference model is given by $p(H|A, X) = p(H|A, X, \mu, \Sigma)$, where μ and Σ are considered as random variables computed by stacked stochastic layers with noise injected to each layer. The marginalized $p(H|A, X)$ is hence not necessarily a Gaussian distribution and enabled higher flexibility and expressivity.

There exist other variations of the variational graph autoencoders such as JTVAE [87] and DGVAE [88]. However, those variational graph autoencoders focus on the generation of graphs. As we mainly consider the learning of representations, we omit the introduction to those methods.

4.1.3 Autoregressive Reconstruction

Following the idea of **GPT** [89] for the generative pre-training of language models, **GPT-GNN** [53] proposes a autoregressive framework to perform reconstruction on given graphs. As both variational autoencoders and the autoregressive models are generative and based on reconstruction, graph autoregressive models differ from that they perform reconstruction iteratively. In particular, GPT-GNN consists

of a graph encoder f , decoders g_n and g_e for node generation and edge generation, respectively. Given a graph with its nodes and edges randomly masked, GPT-GNN generates one masked node and its edges at a time and optimizes the likelihood of the node and edges generated in the current iteration. GPT-GNN iteratively generates nodes and edges until all masked nodes are generated.

4.2 Graph Property Prediction

In addition to the reconstruction, an efficient way to perform self-supervised predictive learning is to design the prediction tasks based on informative graph properties that are not explicitly provided in the graph data. Commonly applied properties for self-supervised training include topology properties, statistical properties, and domain-knowledge involved properties.

S²GRL [54] generalizes the adjacency matrix reconstruction task to a **k -hop connectivity prediction** task between two given nodes, motivated by that the interaction between two nodes is not limited to their direct connection. In particular, given encoded representations of any pair of nodes, the prediction head performs classification on the absolute difference between the representations. S²GRL then trains the encoder and prediction head to classify the hop counts between the pair of nodes.

Meta-path prediction [56] provides a self-supervision for heterogeneous graphs, such as molecules, which include multiple types of nodes and edges. A meta-path of length ℓ is defined as a sequence (t_1, \dots, t_ℓ) where t_i denotes the type of the i -th edge in the path. Given two nodes in a heterogeneous graph and K meta-paths, the encoder f and prediction heads g_i ($i = 1, \dots, K$) are trained to predict if the two nodes are connected by each of the meta-paths as a binary classification task. In [56], the predictions of the K meta-paths are included as K auxiliary learning tasks in addition to the main learning task.

GROVER [55] performs self-supervised learning on molecular graph data with two predictive learning tasks. In **contextual property prediction**, the encoder and prediction head is trained to predict the "atom-bond-count" relationship within the k -hop neighborhood of a given node (atom), e.g. "O-double_bond-2" if there are two atoms "O" connected to the given atom with double bonds. In addition, a **graph-level motif prediction** task is applied to involve the self-supervision of domain knowledge. For molecular graphs, the motifs are instantiated by the functional groups in molecules. Given a list of motifs, the graph-level prediction head predicts the existence of each motif, as a multi-label classification task.

4.3 Multi-Stage Self-Training

Instead of the labels obtained from input graphs, the prediction targets in self-training methods are pseudo-labels obtained from the prediction in a previous stage or even randomly assigned. The self-trained graph neural networks can be either applied under a semi-supervised setting or further fine-tuned for downstream tasks. We consider the node-level classification for an instance.

Under the node-level semi-supervised setting, the **multi-stage self-training** [90] is proposed to utilize the labeled

nodes to guide the training on unlabeled nodes. Concretely, given both the labeled node set and unlabeled node set, the graph neural network is first trained on the labeled set. After the training, it performs prediction on the unlabeled set and the predicted labels with high confidence are considered as the pseudo-labels and moved to the labeled node set. Then a fresh graph neural network is trained on the updated labeled set and the above operations are performed multiple times.

M3S [57] applies DeepCluster [91] and an aligning mechanism to generate pseudo-labels on the basis of multi-stage self-training. In particular, a K -mean cluster is performed on node-level representations at each stage and the labels obtained from clustering are then aligned with the given true labels. A node with clustered pseudo-label is added to the labeled set for self-training in the next stage only if it matches the prediction of the classifier in the current stage. Compared to the basic multi-stage self-training, M3S considers the DeepCluster and the aligning mechanism as a self-checking mechanism and hence provides stronger self-supervision.

A recent study [92] provides the theoretical justification for the self-training with pseudo-labels based on an assumption of the expansion property and generalizes the self-training methods from semi-supervised settings into the unsupervised setting. Intuitively, the examples with correct pseudo-labels will be utilized to denoise the incorrectly pseudo-labeled examples and high accuracy can be achieved due to the expansion assumption. Under the unsupervised setting, it theoretically shows that a classifier trained with arbitrarily assigned pseudo-labels can still achieve good accuracy for some permutation of the classes.

5 SUMMARY OF LEARNING TASKS AND DATASETS

The self-supervised learning methods are usually applied to and evaluated on two common types of graph-related learning tasks, the graph-level inductive learning and the node-level transductive learning. The graph-level inductive learning aims to learn models predicting graph-level properties, and the models are trained and perform prediction on different sets of graphs. On the other hand, the node-level transductive learning aims to learn models performs node-level property prediction, trained and performing prediction on the same sets of large graphs. In this section, we summarize datasets under the two types of learning tasks. The statistics of common datasets are shown in Table 5.

5.1 Graph-Level Inductive Learning

Graph-level learning tasks are performed as inductive learning tasks on multiple graphs [37]. Commonly used datasets for graph-level learning tasks can be divided into three types, chemical molecule datasets, protein datasets, and social network datasets.

Chemical Molecular Property Prediction. In a molecular graph, each node represents an atom in a molecule where the atom index is indicated by the node attribute and each edge represents a bond in the molecule. Datasets for chemical molecular property prediction are also categorized as small molecule datasets in TUDataset [93]. Traditional

TABLE 1

Summary and statistics of common graph datasets for self-supervised learning. Unsupervised classification refers to performing unsupervised representation learning followed by linear classification.

Datasets	Evaluation tasks	Category	# graphs	Avg. nodes	Avg. edges	# classes
NCI1	Unsupervised or semi-supervised learning for graph classification	Small molecules	4110	29.87	32.30	2
MUTAG		Small molecules	1113	17.93	19.79	2
PTC-MR		Small molecules	344	14.29	14.69	2
PROTEINS		Bioinformatics (proteins)	1178	39.06	72.82	2
DD		Bioinformatics (proteins)	188	284.32	715.66	2
BBBP	Unsupervised transfer learning for graph classification	Small molecules	2039	24.05	25.94	2
Tox21		Small molecules	7831	18.51	25.94	12 (multi-label)
ToxCast		Small molecules	8575	18.78	19.26	167 (multi-label)
SIDER		Small molecules	1427	33.64	35.36	27 (multi-label)
ClinTox		Small molecules	1478	26.13	27.86	2
MUV		Small molecules	93087	24.23	26.28	17 (multi-label)
HIV		Small molecules	41127	25.53	27.48	2
BACE		Small molecules	1513	34.12	36.89	2
PPI		Bioinformatics (proteins)	24	56,944	818,716	121 (multi-label)
COLLAB	Unsupervised or semi-supervised learning for graph classification	Social networks	5000	74.49	2457.78	2
RDT-B		Social networks	2000	429.63	497.75	2
RDT-M5K		Social networks	4999	508.52	594.87	5
IMDB-B		Social networks	1000	19.77	96.53	2
CORA	Node clustering, unsupervised classification, or semi-supervised link prediction	Citation network	1	2,708	5,429	7
CITSEER		Citation network	1	3,327	4,732	6
PUBMED		Citation network	1	19,717	44,338	3

molecule classification datasets such as **NCI1** [94] and **MUTAG** [95] are the most commonly used datasets for unsupervised graph representation learning in self-supervision related studies [9, 48]. In addition, the molecule property prediction models can be also trained in a self-supervised pre-training and finetuning fashion for semi-supervised learning and transfer learning. Recent works [42, 48, 55] build their pre-training molecule dataset by sampling unlabeled molecules from the **ZINC15** [96] database containing 750 million molecules. **MoleculeNet** [20] also provides a collection of molecular graph datasets for molecule property prediction, which is suitable for downstream graph classification. Among all the datasets in MoleculeNet, the classification datasets such as **BBBP**, **Tox21**, and **HIV** are used for the evaluation of several self-supervised learning methods [42, 48, 55].

Protein Biological Function Prediction. The protein is a particular type of molecule but is represented differently by graph data. In a protein graph, nodes represent amino acids and an edge indicates the two connected nodes are less than 6 Angstroms apart. Datasets for chemical molecular property prediction are also categorized as bioinformatics datasets in TUDataset. Similar to the chemical molecule datasets, protein datasets can be used in both unsupervised representation learning, such as **PROTEINS** [97] and **DD** [98], and in the two-stage training. For the two-stage training, Hu et al. [42] build their own pre-training dataset containing 395K unlabeled protein obtained from **protein-protein interaction (PPI) networks** [99] and perform finetuning on PPI networks consisting of 88K proteins labeled with 40 fine-grained biological functions, obtained from Zitnik et al. [100].

Social Network Property Prediction. A social network graph dataset considers each entity (e.g. a user or an author) as a node and their social connections as edges. As social networks in different datasets represent differently, social network graph datasets are not typically used for

transfer learning. Social network graph datasets used in recent self-supervised studies [47, 48] are typical datasets for graph classification [101] such as **COLLAB**, **REDDIT-B** and **IMDB-B**.

5.2 Node-Level Transductive Learning

Node-level learning tasks are performed as transductive learning tasks on large graphs [37]. Currently, most node-level learning tasks are performed on citation network datasets [102], including **CORA** [103], **CITSEER** [104] and **PUBMED** [105]. There are three typical ways to use the citation network datasets. Contrastive learning methods [9, 37, 40] are usually evaluated on the social network datasets by performing unsupervised representation learning followed by a linear classification with fixed representations, whereas predictive learning studies usually perform unsupervised representation learning followed by clustering [49, 50] or semi-supervised link prediction [38, 54] on the social network datasets.

6 AN OPEN-SOURCE LIBRARY

We develop an open-source library DIG: Dive into Graphs, which includes a module, known as `sslgraph`¹, for self-supervised learning of GNNs. DIG-`sslgraph` is based on Pytorch [106] and Pytorch Geometric [107] and aims at easy implementation and standardized evaluation of SSL methods for graph neural networks. An overview of the library is shown in Figure 7. In particular, we provide a unified and highly customizable framework for contrastive learning methods, standardized data interface, and evaluation tools that are compatible for evaluating both contrastive methods and predictive methods.

Given the developed unified contrastive framework as a base class, particular contrastive learning methods can

1. The open-source library is now publicly available at the URL: <https://github.com/divelab/DIG/tree/main/dig/sslgraph>.

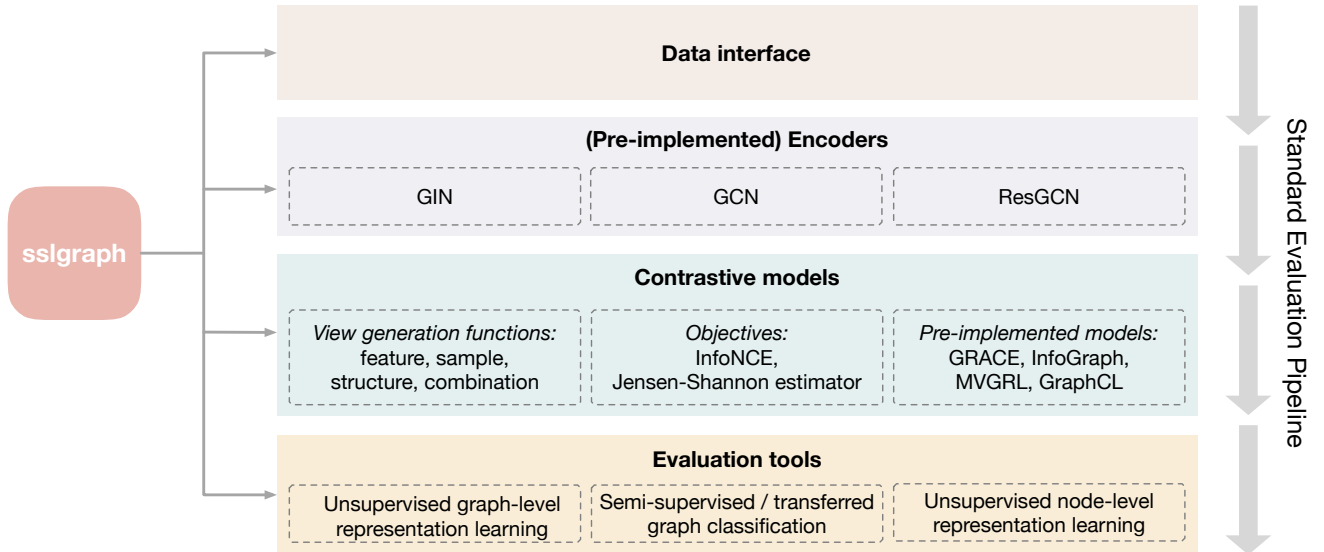


Fig. 7. An overview of the developed sslgraph library within DIG: Dive into Graphs. The library provides a standardized evaluation framework consisting of customizable framework and pre-implemented models for contrastive methods, data interface and evaluation tools for both contrastive and predictive methods.

be easily implemented by specifying their objective, functions for view generation, and their encoders. We also pre-implement four state-of-the-art contrastive methods for either node-level or graph-level tasks based on the unified framework, including InfoGraph [40], GRACE [45], MVGRL [57], and GraphCL [48].

The provided data interface includes datasets from TU-Dataset [93] and the citation network dataset [102]. Other datasets from Pytorch Geometric and new datasets processed by Pytorch Geometric are also supported by our data interface. The provided evaluation tools and data interface allow standardized evaluations of SSL methods and fair comparisons with existing SSL methods under common evaluation settings, including unsupervised graph-level representation learning, semi-supervised graph classification (or transfer learning, depending on the datasets), and unsupervised node-level representation learning. Altogether, our open-source library provides a complete and extensible framework for developing and evaluating SSL methods for GNNs.

7 CONCLUSION

Despite recent successes in natural language processing and computer vision, the self-supervised learning applied to graph data is still an emerging field and has significant challenges to be addressed. Existing methods employ self-supervision to graph neural networks through either contrastive learning or predictive learning. We summarize current self-supervised learning methods and provide unified reviews for the two approaches. We unify existing contrastive learning methods for GNNs with a general contrastive framework, which performs mutual information maximization on different views of given graphs with appropriate MI estimators. We demonstrate that any existing method can be realized by determining its MI estimator, views generation, and graph encoder. We further provide detailed descriptions of existing options for the components

and discussions to guide the choice of those components. For predictive learning, we categorize existing methods into graph reconstruction, property prediction, and self-training based on how labels are generated from the data. A thorough review is provided for methods in all three types of predictive learning. Finally, we summarize common graph datasets of different domains and introduce what learning tasks the datasets are involved in to provide a clear view to conduct future evaluation experiments. Altogether, our unified treatment of SSL in GNNs in terms of methodologies, datasets, evaluations, and open-source software is anticipated to foster methodological developments and facilitate empirical comparisons.

ACKNOWLEDGMENTS

This work was supported in part by National Science Foundation grants IIS-2006861 and DBI-2028361, and National Institutes of Health grant 1R21NS102828. We thank the scientific community for providing valuable feedback and comments, which lead to improvements of this work.

REFERENCES

- [1] D. Ulyanov, A. Vedaldi, and V. Lempitsky, “Deep image prior,” in *Proceedings of the IEEE Conference on Computer Vision and Pattern Recognition*, June 2018.
- [2] Y. Xie, Z. Wang, and S. Ji, “Noise2Same: Optimizing a self-supervised bound for image denoising,” in *Advances in Neural Information Processing Systems*, vol. 33, 2020, pp. 20 320–20 330.
- [3] S. Laine, T. Karras, J. Lehtinen, and T. Aila, “High-quality self-supervised deep image denoising,” *Advances in Neural Information Processing Systems*, vol. 32, pp. 6970–6980, 2019.
- [4] A. Krull, T.-O. Buchholz, and F. Jug, “Noise2Void-learning denoising from single noisy images,” in *Proceedings of the IEEE Conference on Computer Vision and Pattern Recognition*, 2019, pp. 2129–2137.

- [5] J. Batson and L. Royer, "Noise2Self: Blind denoising by self-supervision," in *Proceedings of the 36th International Conference on Machine Learning*, vol. 97, 2019, pp. 524–533.
- [6] J. Devlin, M. Chang, K. Lee, and K. Toutanova, "BERT: pre-training of deep bidirectional transformers for language understanding," in *Proceedings of the 2019 Conference of the North American Chapter of the Association for Computational Linguistics: Human Language Technologies*, 2019, pp. 4171–4186.
- [7] J. Wu, X. Wang, and W. Y. Wang, "Self-supervised dialogue learning," in *Proceedings of the 57th Annual Meeting of the Association for Computational Linguistics*, 2019, pp. 3857–3867.
- [8] H. Wang, X. Wang, W. Xiong, M. Yu, X. Guo, S. Chang, and W. Y. Wang, "Self-supervised learning for contextualized extractive summarization," in *Proceedings of the 57th Annual Meeting of the Association for Computational Linguistics*, 2019, pp. 2221–2227.
- [9] K. Hassani and A. H. Khasahmadi, "Contrastive multi-view representation learning on graphs," in *Proceedings of the 37th International Conference on Machine Learning*, 2020.
- [10] T. Chen, S. Kornblith, M. Norouzi, and G. Hinton, "A simple framework for contrastive learning of visual representations," in *Proceedings of the International Conference on Machine Learning*, 2020.
- [11] A. v. d. Oord, Y. Li, and O. Vinyals, "Representation learning with contrastive predictive coding," *arXiv preprint arXiv:1807.03748*, 2018.
- [12] Y. Tian, D. Krishnan, and P. Isola, "Contrastive multi-view coding," *arXiv preprint arXiv:1906.05849*, 2019.
- [13] B. Perozzi, R. Al-Rfou, and S. Skiena, "Deepwalk: On-line learning of social representations," in *Proceedings of the 20th ACM SIGKDD International Conference on Knowledge Discovery and Data Mining*, ser. KDD '14, 2014, pp. 701–710.
- [14] A. Narayanan, M. Chandramohan, R. Venkatesan, L. Chen, Y. Liu, and S. Jaiswal, "graph2vec: Learning distributed representations of graphs," *arXiv preprint arXiv:1707.05005*, 2017.
- [15] A. Tsitsulin, D. Mottin, P. Karras, A. Bronstein, and E. Müller, "Sgr: Self-supervised spectral graph representation learning," *arXiv preprint arXiv:1811.06237*, 2018.
- [16] C. Doersch, A. Gupta, and A. A. Efros, "Unsupervised visual representation learning by context prediction," in *Proceedings of the IEEE international conference on computer vision*, 2015, pp. 1422–1430.
- [17] M. Noroozi and P. Favaro, "Unsupervised learning of visual representations by solving jigsaw puzzles," in *European conference on computer vision*. Springer, 2016, pp. 69–84.
- [18] K. He, H. Fan, Y. Wu, S. Xie, and R. Girshick, "Momentum contrast for unsupervised visual representation learning," in *Proceedings of the IEEE Conference on Computer Vision and Pattern Recognition*, 2020.
- [19] J.-B. Grill, F. Strub, F. Altché, C. Tallec, P. Richemond, E. Buchatskaya, C. Doersch, B. Avila Pires, Z. Guo, M. Gheshlaghi Azar, B. Piot, k. kavukcuoglu, R. Munos, and M. Valko, "Bootstrap your own latent - a new approach to self-supervised learning," in *Advances in Neural Information Processing Systems*, vol. 33, 2020, pp. 21 271–21 284.
- [20] Z. Wu, B. Ramsundar, E. N. Feinberg, J. Gomes, C. Geniesse, A. S. Pappu, K. Leswing, and V. Pande, "Moleculenet: a benchmark for molecular machine learning," *Chemical Science*, vol. 9, no. 2, pp. 513–530, 2018.
- [21] Z. Wang, M. Liu, Y. Luo, Z. Xu, Y. Xie, L. Wang, L. Cai, and S. Ji, "Advanced graph and sequence neural networks for molecular property prediction and drug discovery," *arXiv preprint arXiv:2012.01981*, 2020.
- [22] T. N. Kipf and M. Welling, "Semi-supervised classification with graph convolutional networks," in *International Conference on Learning Representations*, 2017.
- [23] K. Xu, W. Hu, J. Leskovec, and S. Jegelka, "How powerful are graph neural networks?" in *International Conference on Learning Representations*, 2019. [Online]. Available: <https://openreview.net/forum?id=ryGs6iA5Km>
- [24] H. Gao and S. Ji, "Graph U-Nets," in *Proceedings of the 36th International Conference on Machine Learning*, 2019, pp. 2083–2092.
- [25] M. Liu, Z. Wang, and S. Ji, "Non-local graph neural networks," *arXiv preprint arXiv:2005.14612*, 2020.
- [26] L. Cai, J. Li, J. Wang, and S. Ji, "Line graph neural networks for link prediction," *arXiv preprint arXiv:2010.10046*, 2020.
- [27] M. Liu, H. Gao, and S. Ji, "Towards deeper graph neural networks," in *Proceedings of the 26th ACM SIGKDD International Conference on Knowledge Discovery and Data Mining*, 2020, pp. 338–348.
- [28] L. Cai and S. Ji, "A multi-scale approach for graph link prediction," in *Proceedings of the 34th AAAI Conference on Artificial Intelligence*, 2020, pp. 3308–3315.
- [29] H. Gao, Z. Wang, and S. Ji, "Large-scale learnable graph convolutional networks," in *Proceedings of the 24th ACM SIGKDD International Conference on Knowledge Discovery and Data Mining*, 2018, pp. 1416–1424.
- [30] H. Gao, Y. Chen, and S. Ji, "Learning graph pooling and hybrid convolutional operations for text representations," in *Proceedings of the Web Conference*, 2019, pp. 2743–2749.
- [31] H. Gao, Y. Liu, and S. Ji, "Topology-aware graph pooling networks," *arXiv preprint arXiv:2010.09834*, 2020.
- [32] Z. Wang and S. Ji, "Second-order pooling for graph neural networks," *IEEE Transactions on Pattern Analysis and Machine Intelligence*, 2020.
- [33] H. Yuan and S. Ji, "StructPool: Structured graph pooling via conditional random fields," in *Proceedings of the 8th International Conference on Learning Representations*, 2020.
- [34] H. Gao and S. Ji, "Graph representation learning via hard and channel-wise attention networks," in *Proceedings of the 25th ACM SIGKDD International Conference on Knowledge Discovery & Data Mining*. ACM, 2019, pp. 741–749.
- [35] H. Yuan, J. Tang, X. Hu, and S. Ji, "XGNN: Towards model-level explanations of graph neural networks," in *Proceedings of the 26th ACM SIGKDD International*

- Conference on Knowledge Discovery and Data Mining*, 2020, pp. 430–438.
- [36] Y. Liu, H. Yuan, L. Cai, and S. Ji, “Deep learning of high-order interactions for protein interface prediction,” in *Proceedings of the 26th ACM SIGKDD International Conference on Knowledge Discovery and Data Mining*, 2020, pp. 679–687.
- [37] P. Veličković, W. Fedus, W. L. Hamilton, P. Liò, Y. Bengio, and D. Hjelm, “Deep graph infomax,” in *International Conference on Learning Representations*, 2019.
- [38] T. N. Kipf and M. Welling, “Variational graph auto-encoders,” *arXiv preprint arXiv:1611.07308*, 2016.
- [39] Y. Ma and J. Tang, *Deep Learning on Graphs*. Cambridge University Press, 2020.
- [40] F.-Y. Sun, J. Hoffman, V. Verma, and J. Tang, “Infograph: Unsupervised and semi-supervised graph-level representation learning via mutual information maximization,” in *International Conference on Learning Representations*, 2019.
- [41] Z. Peng, W. Huang, M. Luo, Q. Zheng, Y. Rong, T. Xu, and J. Huang, “Graph representation learning via graphical mutual information maximization,” in *Proceedings of The Web Conference 2020*, 2020, pp. 259–270.
- [42] W. Hu, B. Liu, J. Gomes, M. Zitnik, P. Liang, V. Pande, and J. Leskovec, “Strategies for pre-training graph neural networks,” in *International Conference on Learning Representations*, 2020. [Online]. Available: <https://openreview.net/forum?id=HJIWWJSFDH>
- [43] Y. Jiao, Y. Xiong, J. Zhang, Y. Zhang, T. Zhang, and Y. Zhu, “Sub-graph contrast for scalable self-supervised graph representation learning,” *arXiv preprint arXiv:2009.10273*, 2020.
- [44] Y. Zhu, Y. Xu, F. Yu, Q. Liu, S. Wu, and L. Wang, “Graph contrastive learning with adaptive augmentation,” in *Proceedings of The Web Conference 2021*, ser. WWW ’21, 2021.
- [45] —, “Deep graph contrastive representation learning,” *arXiv preprint arXiv:2006.04131*, 2020.
- [46] S. Thakoor, C. Tallec, M. G. Azar, R. Munos, P. Veličković, and M. Valko, “Bootstrapped representation learning on graphs,” *arXiv preprint arXiv:2102.06514*, 2021.
- [47] J. Qiu, Q. Chen, Y. Dong, J. Zhang, H. Yang, M. Ding, K. Wang, and J. Tang, “GCC: Graph contrastive coding for graph neural network pre-training,” in *Proceedings of the 26th ACM SIGKDD International Conference on Knowledge Discovery & Data Mining*, 2020, pp. 1150–1160.
- [48] Y. You, T. Chen, Y. Sui, T. Chen, Z. Wang, and Y. Shen, “Graph contrastive learning with augmentations,” in *Advances in Neural Information Processing Systems*, vol. 33, 2020, pp. 5812–5823.
- [49] C. Wang, S. Pan, G. Long, X. Zhu, and J. Jiang, “Mgae: Marginalized graph autoencoder for graph clustering,” in *Proceedings of the 2017 ACM on Conference on Information and Knowledge Management*, 2017, pp. 889–898.
- [50] J. Park, M. Lee, H. J. Chang, K. Lee, and J. Y. Choi, “Symmetric graph convolutional autoencoder for unsupervised graph representation learning,” in *Proceedings of the IEEE/CVF International Conference on Computer Vision*, 2019, pp. 6519–6528.
- [51] S. Pan, R. Hu, G. Long, J. Jiang, L. Yao, and C. Zhang, “Adversarially regularized graph autoencoder for graph embedding,” in *Proceedings of the 27th International Joint Conference on Artificial Intelligence*, 2018, pp. 2609–2615.
- [52] A. Hasanzadeh, E. Hajiramezanali, K. Narayanan, N. Duffield, M. Zhou, and X. Qian, “Semi-implicit graph variational auto-encoders,” in *Advances in Neural Information Processing Systems*, vol. 32, 2019, pp. 10712–10723.
- [53] Z. Hu, Y. Dong, K. Wang, K.-W. Chang, and Y. Sun, “Gpt-gnn: Generative pre-training of graph neural networks,” in *Proceedings of the 26th ACM SIGKDD International Conference on Knowledge Discovery & Data Mining*, 2020, pp. 1857–1867.
- [54] Z. Peng, Y. Dong, M. Luo, X.-M. Wu, and Q. Zheng, “Self-supervised graph representation learning via global context prediction,” *arXiv preprint arXiv:2003.01604*, 2020.
- [55] Y. Rong, Y. Bian, T. Xu, W. Xie, Y. Wei, W. Huang, and J. Huang, “Self-supervised graph transformer on large-scale molecular data,” in *Advances in Neural Information Processing Systems*, 2020.
- [56] D. Hwang, J. Park, S. Kwon, K.-M. Kim, J.-W. Ha, and H. J. Kim, “Self-supervised auxiliary learning with meta-paths for heterogeneous graphs,” *arXiv preprint arXiv:2007.08294*, 2020.
- [57] K. Sun, Z. Lin, and Z. Zhu, “Multi-stage self-supervised learning for graph convolutional networks on graphs with few labeled nodes,” in *Proceedings of the AAAI Conference on Artificial Intelligence*, vol. 34, no. 04, 2020, pp. 5892–5899.
- [58] W. Jin, T. Derr, H. Liu, Y. Wang, S. Wang, Z. Liu, and J. Tang, “Self-supervised learning on graphs: Deep insights and new direction,” *arXiv preprint arXiv:2006.10141*, 2020.
- [59] Y. Ganin and V. Lempitsky, “Unsupervised domain adaptation by backpropagation,” in *International Conference on Machine Learning*. PMLR, 2015, pp. 1180–1189.
- [60] Y. Sun, E. Tzeng, T. Darrell, and A. A. Efros, “Unsupervised domain adaptation through self-supervision,” *arXiv preprint arXiv:1909.11825*, 2019.
- [61] R. D. Hjelm, A. Fedorov, S. Lavoie-Marchildon, K. Grewal, P. Bachman, A. Trischler, and Y. Bengio, “Learning deep representations by mutual information estimation and maximization,” in *International Conference on Learning Representations*, 2019. [Online]. Available: <https://openreview.net/forum?id=Bklr3j0cKX>
- [62] M. D. Donsker and S. R. S. Varadhan, “Asymptotic evaluation of certain markov process expectations for large time. iv,” *Communications on Pure and Applied Mathematics*, vol. 36, pp. 183–212, 1983.
- [63] M. I. Belghazi, A. Baratin, S. Rajeshwar, S. Ozair, Y. Bengio, A. Courville, and D. Hjelm, “Mutual information neural estimation,” in *Proceedings of the 35th International Conference on Machine Learning*, vol. 80. PMLR, 2018, pp. 531–540.

- [64] S. Nowozin, B. Cseke, and R. Tomioka, "f-gan: Training generative neural samplers using variational divergence minimization," in *Advances in Neural Information Processing Systems*, 2016, pp. 271–279.
- [65] M. Gutmann and A. Hyvärinen, "Noise-contrastive estimation: A new estimation principle for unnormalized statistical models," in *Proceedings of the Thirteenth International Conference on Artificial Intelligence and Statistics*, 2010, pp. 297–304.
- [66] K. Sohn, "Improved deep metric learning with multi-class n-pair loss objective," in *Advances in Neural Information Processing Systems*, vol. 29, 2016, pp. 1857–1865.
- [67] S. Rendle, C. Freudenthaler, Z. Gantner, and L. Schmidt-Thieme, "Bpr: Bayesian personalized ranking from implicit feedback," in *Proceedings of the Twenty-Fifth Conference on Uncertainty in Artificial Intelligence*, 2009, p. 452–461.
- [68] F. Schroff, D. Kalenichenko, and J. Philbin, "Facenet: A unified embedding for face recognition and clustering," in *Proceedings of the IEEE Conference on Computer Vision and Pattern Recognition*, 2015, pp. 815–823.
- [69] E. Hoffer and N. Ailon, "Deep metric learning using triplet network," in *International workshop on similarity-based pattern recognition*. Springer, 2015, pp. 84–92.
- [70] T. Mikolov, K. Chen, G. Corrado, and J. Dean, "Efficient estimation of word representations in vector space," in *1st International Conference on Learning Representations, Workshop Track Proceedings*, 2013.
- [71] Y. Tian, C. Sun, B. Poole, D. Krishnan, C. Schmid, and P. Isola, "What makes for good views for contrastive learning?" *arXiv preprint arXiv:2005.10243*, 2020.
- [72] C. Wei, K. Shen, Y. Chen, and T. Ma, "Theoretical analysis of self-training with deep networks on unlabeled data," *arXiv preprint arXiv:2010.03622*, 2020.
- [73] P. Veličković, G. Cucurull, A. Casanova, A. Romero, P. Liò, and Y. Bengio, "Graph attention networks," in *International Conference on Learning Representations*, 2018. [Online]. Available: <https://openreview.net/forum?id=rJXMpikCZ>
- [74] K. Xu, C. Li, Y. Tian, T. Sonobe, K.-i. Kawarabayashi, and S. Jegelka, "Representation learning on graphs with jumping knowledge networks," in *International Conference on Machine Learning*. PMLR, 2018, pp. 5453–5462.
- [75] D. Erhan, Y. Bengio, A. Courville, P.-A. Manzagol, P. Vincent, and S. Bengio, "Why does unsupervised pre-training help deep learning?" *Journal of Machine Learning Research*, vol. 11, no. 19, pp. 625–660, 2010. [Online]. Available: <http://jmlr.org/papers/v11/erhan10a.html>
- [76] M. Tschannen, J. Djolonga, P. K. Rubenstein, S. Gelly, and M. Lucic, "On mutual information maximization for representation learning," in *International Conference on Learning Representations*, 2020. [Online]. Available: <https://openreview.net/forum?id=rkxoh24FPH>
- [77] X. Liu, F. Zhang, Z. Hou, Z. Wang, L. Mian, J. Zhang, and J. Tang, "Self-supervised learning: Generative or contrastive," *arXiv preprint arXiv:2006.08218*, vol. 1, no. 2, 2020.
- [78] M. A. Kramer, "Nonlinear principal component analysis using autoassociative neural networks," *AIChE journal*, vol. 37, no. 2, pp. 233–243, 1991.
- [79] W. L. Hamilton, "Graph representation learning," *Synthesis Lectures on Artificial Intelligence and Machine Learning*, vol. 14, no. 3, pp. 1–159.
- [80] W. Hamilton, Z. Ying, and J. Leskovec, "Inductive representation learning on large graphs," in *Advances in Neural Information Processing Systems*, 2017, pp. 1024–1034.
- [81] D. Kim and A. Oh, "How to find your friendly neighborhood: Graph attention design with self-supervision," in *International Conference on Learning Representations*, 2021. [Online]. Available: <https://openreview.net/forum?id=Wi5KUNlqWty>
- [82] W. Jin, T. Derr, Y. Wang, Y. Ma, Z. Liu, and J. Tang, "Node similarity preserving graph convolutional networks," 2020.
- [83] P. Vincent, H. Larochelle, I. Lajoie, Y. Bengio, P.-A. Manzagol, and L. Bottou, "Stacked denoising autoencoders: Learning useful representations in a deep network with a local denoising criterion." *Journal of Machine Learning Research*, vol. 11, no. 12, 2010.
- [84] G. Taubin, "A signal processing approach to fair surface design," in *Proceedings of the 22nd annual conference on Computer graphics and interactive techniques*, 1995, pp. 351–358.
- [85] Y. You, T. Chen, Z. Wang, and Y. Shen, "When does self-supervision help graph convolutional networks?" in *International Conference on Machine Learning*. PMLR, 2020, pp. 10 871–10 880.
- [86] I. Goodfellow, J. Pouget-Abadie, M. Mirza, B. Xu, D. Warde-Farley, S. Ozair, A. Courville, and Y. Bengio, "Generative adversarial nets," in *Advances in Neural Information Processing Systems*, vol. 27, 2014, pp. 2672–2680.
- [87] W. Jin, R. Barzilay, and T. Jaakkola, "Junction tree variational autoencoder for molecular graph generation," in *International Conference on Machine Learning*. PMLR, 2018, pp. 2323–2332.
- [88] J. Li, T. Y. J. Li, H. Zhang, K. Zhao, Y. Rong, and H. Cheng, "Dirichlet graph variational autoencoder," in *Advances in Neural Information Processing Systems*, 2020.
- [89] A. Radford, J. Wu, R. Child, D. Luan, D. Amodei, and I. Sutskever, "Language models are unsupervised multitask learners," 2019. [Online]. Available: <https://d4mucfpksywv.cloudfront.net/better-language-models/language-models.pdf>
- [90] Q. Li, Z. Han, and X.-M. Wu, "Deeper insights into graph convolutional networks for semi-supervised learning," in *Proceedings of the AAAI Conference on Artificial Intelligence*, vol. 32, no. 1, 2018.
- [91] M. Caron, P. Bojanowski, A. Joulin, and M. Douze, "Deep clustering for unsupervised learning of visual features," in *Proceedings of the European Conference on Computer Vision (ECCV)*, 2018, pp. 132–149.
- [92] C. Wei, K. Shen, Y. Chen, and T. Ma, "Theoretical analysis of self-training with deep networks on unlabeled data," in *International Conference on Learning Representations*, 2021. [Online]. Available: <https://openreview.net/forum?id=rC8sJ4i6kaH>
- [93] C. Morris, N. M. Kriege, F. Bause, K. Kersting,

- P. Mutzel, and M. Neumann, "Tudataset: A collection of benchmark datasets for learning with graphs," in *ICML 2020 Workshop on Graph Representation Learning and Beyond (GRL+ 2020)*, 2020. [Online]. Available: www.graphlearning.io
- [94] N. Wale and G. Karypis, "Comparison of descriptor spaces for chemical compound retrieval and classification," in *Sixth International Conference on Data Mining (ICDM'06)*, 2006, pp. 678–689.
- [95] A. K. Debnath, R. L. Lopez de Compadre, G. Debnath, A. J. Shusterman, and C. Hansch, "Structure-activity relationship of mutagenic aromatic and heteroaromatic nitro compounds correlation with molecular orbital energies and hydrophobicity," *Journal of Medicinal Chemistry*, vol. 34, no. 2, pp. 786–797, 02 1991.
- [96] T. Sterling and J. J. Irwin, "Zinc 15–ligand discovery for everyone," *Journal of Chemical Information and Modeling*, vol. 55, no. 11, pp. 2324–2337, 2015.
- [97] K. M. Borgwardt, C. S. Ong, S. Schönauer, S. V. N. Vishwanathan, A. J. Smola, and H.-P. Kriegel, "Protein function prediction via graph kernels," *Bioinformatics*, vol. 21, pp. i47–i56, 06 2005.
- [98] P. D. Dobson and A. J. Doig, "Distinguishing enzyme structures from non-enzymes without alignments," *Journal of Molecular Biology*, vol. 330, no. 4, pp. 771–783, 2003.
- [99] M. Zitnik and J. Leskovec, "Predicting multicellular function through multi-layer tissue networks," *Bioinformatics*, vol. 33, no. 14, pp. i190–i198, 2017.
- [100] M. Zitnik, M. W. Feldman, J. Leskovec *et al.*, "Evolution of resilience in protein interactomes across the tree of life," *Proceedings of the National Academy of Sciences*, vol. 116, no. 10, pp. 4426–4433, 2019.
- [101] P. Yanardag and S. Vishwanathan, "Deep graph kernels," in *Proceedings of the 21th ACM SIGKDD International Conference on Knowledge Discovery and Data Mining*, 2015, p. 1365–1374.
- [102] Z. Yang, W. Cohen, and R. Salakhudinov, "Revisiting semi-supervised learning with graph embeddings," in *International conference on machine learning*. PMLR, 2016, pp. 40–48.
- [103] A. K. McCallum, K. Nigam, J. Rennie, and K. Seymore, "Automating the construction of internet portals with machine learning," *Information Retrieval*, vol. 3, no. 2, pp. 127–163, 2000.
- [104] C. L. Giles, K. D. Bollacker, and S. Lawrence, "Citeseer: An automatic citation indexing system," in *Proceedings of the Third ACM Conference on Digital Libraries*. Association for Computing Machinery, 1998, p. 89–98.
- [105] P. Sen, G. Namata, M. Bilgic, L. Getoor, B. Galligher, and T. Eliassi-Rad, "Collective classification in network data," *AI magazine*, vol. 29, no. 3, pp. 93–93, 2008.
- [106] A. Paszke, S. Gross, F. Massa, A. Lerer, J. Bradbury, G. Chanan, T. Killeen, Z. Lin, N. Gimeshein, L. Antiga, A. Desmaison, A. Kopf, E. Yang, Z. DeVito, M. Raison, A. Tejani, S. Chilamkurthy, B. Steiner, L. Fang, J. Bai, and S. Chintala, "Pytorch: An imperative style, high-performance deep learning library," in *Advances in Neural Information Processing Systems 32*, 2019, pp. 8024–8035.
- [107] M. Fey and J. E. Lenssen, "Fast graph representation learning with PyTorch Geometric," in *ICLR Workshop on Representation Learning on Graphs and Manifolds*, 2019.